



THE UNIVERSITY *of* EDINBURGH

Edinburgh Research Explorer

Vasopressin casts light on the suprachiasmatic nucleus

Citation for published version:

Tsuji, T, Allchorne, AJ, Zhang, M, Tsuji, C, Tobin, VA, Pineda, R, Raftogianni, A, Stern, JE, Grinevich, V, Leng, G & Ludwig, M 2017, 'Vasopressin casts light on the suprachiasmatic nucleus', *Journal of Physiology*.
<https://doi.org/10.1113/JP274025>

Digital Object Identifier (DOI):

[10.1113/JP274025](https://doi.org/10.1113/JP274025)

Link:

[Link to publication record in Edinburgh Research Explorer](#)

Document Version:

Peer reviewed version

Published In:

Journal of Physiology

General rights

Copyright for the publications made accessible via the Edinburgh Research Explorer is retained by the author(s) and / or other copyright owners and it is a condition of accessing these publications that users recognise and abide by the legal requirements associated with these rights.

Take down policy

The University of Edinburgh has made every reasonable effort to ensure that Edinburgh Research Explorer content complies with UK legislation. If you believe that the public display of this file breaches copyright please contact openaccess@ed.ac.uk providing details, and we will remove access to the work immediately and investigate your claim.



Vasopressin casts light on the suprachiasmatic nucleus.

Takahiro Tsuji¹, Andrew J. Allchorne¹, Meng Zhang², Chiharu Tsuji¹, Vicky A. Tobin¹,
Rafael Pineda¹, Androniki Raftogianni³, Javier E. Stern², Valery Grinevich³, Gareth Leng¹
and Mike Ludwig¹

¹*Centre for Integrative Physiology, University of Edinburgh, Edinburgh, UK,*

²*Department of Physiology, Augusta University, Augusta GA USA*

³*Schaller Research Group on Neuropeptides, German Cancer Research Center DKFZ,
Central Institute of Mental Health, and University of Heidelberg, Heidelberg, Germany*

Correspondence should be addressed to: Mike Ludwig

Centre for Integrative Physiology, University of Edinburgh, Hugh Robson Bldg, George
Square, Edinburgh EH8 9XD, UK

Tel: -44 (0) 131 650 3275; Fax: -44 (0) 131 650 2872; email: mike.ludwig@ed.ac.uk

Abstract

In all animals, the transition between night and day engages a host of physiological and behavioural rhythms. These rhythms depend not on the rods and cones of the retina, but on retinal ganglion cells (RGCs) that detect the ambient light level in the environment. These project to the suprachiasmatic nucleus (SCN) of the hypothalamus to entrain circadian rhythms that are generated within the SCN. The neuropeptide vasopressin has an important role in this entrainment. Many SCN neurons express vasopressin, and it has been assumed that the role of vasopressin in the SCN reflects the activity of these cells. Here we show that vasopressin is also expressed in many retinal cells that project to the SCN. Light-evoked vasopressin release contributes to the responses of SCN neurons to light, and enhances expression of the immediate early gene *c-fos* in the SCN, which is involved in photic entrainment of circadian rhythms.

Key points

- A subpopulation of retinal ganglion cells expresses the neuropeptide vasopressin
- These retinal ganglion cells project predominately to our biological clock, the SCN
- Light-induced vasopressin release enhances the responses of SCN neurons to light.

- 34 • It also enhances expression of genes involved in photo-entrainment of biological
35 rhythms

36

37 **Abbreviations:** BSA, bovine serum albumin; CSF, cerebrospinal fluid; DABCO, 1,4-
38 diazabicyclo[2.2.2]octane; DAPI, 4',6-diamidino-2-phenylindole; eGFP, enhanced green
39 fluorescent protein RGCs; retinal ganglion cells; GRP, gastrin-releasing peptide; IGL,
40 intergeniculate leaflet; Opt, olivary pretectal nucleus; PFA, paraformaldehyde; RIA,
41 radioimmunoassay; rAVV, recombinant adeno-associated virus; RHT, retino-hypothalamic
42 tract; SCN, suprachiasmatic nucleus; VP-RGCs, vasopressin-expressing retinal ganglion
43 cells; V1a, vasopressin receptor antagonist ($d(\text{CH}_2)_5\text{Tyr}(\text{Me})_2\text{AVP}$); vGLUT-2, vesicle
44 glutamate transporter 2; VIP, vasoactive intestinal polypeptide; ZT, Zeitgeber time;

45

46 **Competing Interests Statement:** The authors declare that there are no conflicts of interest.

47

48 **Funding information:** Supported by grants from the Biotechnology and Biological Research
49 Council (BB/J004723/1) and Medical Research Council (MR/M022838/1) (ML, GL),
50 National Institute of Health (RO1HL11225) (JES), Chica and Heinz Schaller Research
51 Foundation (VG), fellowships from the Japanese Society for the Promotion of Science (TT,
52 CT), the Newton International Fellowship program (RP), and a Royal Society of Edinburgh
53 travel grant to VG and ML.

54

55 **Acknowledgements:** We thank R. Landgraf (RIAGnosis, Germany) for measuring
56 vasopressin content in the microdialysates; H. Gainer (Bethesda, USA) for vasopressin
57 antibodies; M. Manning (Toledo, OH, USA) for his vasopressin receptor antagonist; Y. Ueta
58 (Kitakyushu, Japan) for the vasopressin-eGFP and A. Kubasik-Thayil (IMPACT Imaging
59 facility, Edinburgh) for technical assistance with confocal microscopy.

60

61 **Author Contributions:** ML, GL, Conception and design, Acquisition of data, Analysis and
62 interpretation of data, Drafting or revising the article; VG, JES Conception and design,
63 Analysis and interpretation of data; TT, AJA, MZ, CT, VAT, RP, AR, Acquisition of data,
64 Analysis and interpretation of data.

65

66

67 **Introduction**

68 The suprachiasmatic nucleus (SCN) of the hypothalamus is the circadian pacemaker
69 of the mammalian brain, orchestrating diurnal cycles in activity, hormone secretion and other
70 physiological variables (Reppert & Weaver, 2002; Hastings *et al.*, 2003; Froy, 2011;
71 Albrecht, 2012) according to an intrinsic circadian rhythmicity of neuronal activity and gene
72 expression. Light entrains the endogenous oscillator in the SCN, synchronizing it with the
73 day-night cycle (Golombek & Rosenstein, 2010), and in mammals information about ambient
74 light intensity originates from a small subset of retinal ganglion cells (RGCs) that are
75 intrinsically photosensitive (Masland, 2001; Hattar *et al.*, 2002; Schmidt *et al.*, 2011), rather
76 than from the rods and cones that are responsible for visual imaging. These intrinsically
77 photosensitive RGCs express the photopigment melanopsin (Lucas, 2013), and use the
78 neurotransmitter glutamate (Marc & Jones, 2002); they project to the SCN to mediate
79 circadian photoentrainment. This neural circuit is independent of conventional retinal
80 phototransduction, since photic entrainment persists in functionally blind transgenic mice
81 lacking rods and cones (Berson *et al.*, 2002).

82 Changes in day length require progressive adjustments of circadian rhythms, but it
83 would be counter-adaptive to reset a rhythm to *any* unexpected light signal. Our experience
84 of jet-lag reflects the resistance of our bodily rhythms to abrupt changes (LeGates *et al.*,
85 2014). Accordingly, in animals, a flash of light close to the end of the night is more likely to
86 result in a phase shift of circadian rhythms than one given earlier. Such light pulses induce
87 expression of a set of immediate-early genes in the SCN, and the ability of light to re-entrain
88 circadian rhythms correlates well with the induction of these genes (Rusak *et al.*, 1993;
89 Kornhauser *et al.*, 1996; Porterfield & Mintz, 2009). Thus a key question is, *how can a light*
90 *pulse trigger gene expression and re-entrain circadian rhythms at some times but not at*
91 *others?* Because the neurones in the SCN display circadian rhythms in gene expression that
92 are maintained even in constant darkness, one possible answer is that these genes regulate
93 intrinsic neuronal excitability, with the consequence that the SCN neurons are only fully
94 responsive to light signals at certain stages of the light-dark cycle. Recent findings indicate
95 that the neuropeptide vasopressin may have a critical role in this process. Transgenic
96 vasopressin V1a receptor knockout mice show damped circadian activity rhythms (Li *et al.*,
97 2009), and, interestingly, such mice are resistant to ‘jet lag’. In these mice, light pulses
98 immediately re-entrain circadian rhythms (Yamaguchi *et al.*, 2013).

99 Vasopressin is involved in diverse physiological and behavioural processes;
100 vasopressin secreted from the pituitary gland is essential for fluid and electrolyte balance,

101 while vasopressin released within the brain has many other roles, including in social
102 behaviour, aggression, and in behavioural rhythms (Bielsky *et al.*, 2005; Ludwig & Leng,
103 2006; Donaldson & Young, 2008; Mieda *et al.*, 2015). Vasopressin is expressed in the
104 dorsomedial SCN, and is an important output; its secretion into the cerebrospinal fluid (CSF)
105 peaks in the early morning and declines by late afternoon (Kalsbeek *et al.*, 2010). The targets
106 for vasopressin released from the SCN include vasopressin cells in other parts of the
107 hypothalamus, including those in the supraoptic and paraventricular nuclei that regulate
108 diverse physiological processes including water intake (Gizowski *et al.*, 2016) and
109 behaviours (Trudel & Bourque, 2010).

110 The vasopressin cells in the dorsomedial SCN are not direct recipients of retinal
111 signals; most of the projections from the retina innervate the ventrolateral SCN, which
112 contains other neuropeptides, including vasoactive intestinal peptide and gastrin-releasing
113 peptide (Antle *et al.*, 2009). Here we show that neurons in the ventrolateral SCN are densely
114 innervated by vasopressin-expressing retinal ganglion cells (VP-RGCs), and that more
115 vasopressin is released in response to light at the end of subjective night than at the end of
116 subjective day. Thus neurons in the ventrolateral SCN both control the output of vasopressin
117 from the SCN by their innervation of vasopressin cells in the dorsomedial SCN, and are
118 themselves regulated by vasopressin inputs from the retina.

119

120 **Material & Methods**

121 *Ethical Approval*

122 Procedures conducted in the UK were approved by the local Ethics Committee and
123 the UK Home Office under the Animals Scientific Procedures Act 1986. Experiments in
124 Germany were approved by the Committee on Animal Health and Care of the local
125 governmental body and performed in strict compliance with the EEC recommendations for
126 the care and the use of laboratory animals (86/609/CEE). Experiments in the USA were
127 performed according to institutional guidelines and approval by the Animal Care and Use
128 Committees of the Georgia Regents University.

129

130 *Animals*

131 Experiments were performed on adult male and female wild-type Sprague-Dawley
132 and transgenic rats (250-350g), housed under controlled conditions (12h light: 12h dark,
133 21°C) with free access to food and water. Most of the immunohistochemistry was carried out
134 on a homozygous line of transgenic rats expressing a vasopressin-eGFP (enhanced green

135 fluorescent protein) fusion gene (Ueta et al., 2005).

136

137 *PCR*

138 22-week old female wild-type rats were used to collect supraoptic nucleus and retina
139 tissue. Total RNA was isolated using TRIzol Reagent (Life Technologies, Carlsbad, CA
140 USA). cDNA was synthesised from 1.5µg of total RNA using the Transcriptor High Fidelity
141 cDNA Synthesis Kit (Roche Diagnostics GmbH, Mannheim Germany) according to the
142 manufacturer's protocol. The PCR was carried out in a 25-µl reaction volume using Go Taq
143 G2 Green Master Mix (Promega Corporation, Madison, WI, USA) and 5, 1, or 0.1µl of
144 cDNA solution were used in each reaction mixture. PCR was performed on a Gene Amp PCR
145 System 9700 (Life Technologies, Carlsbad, CA USA) using the following conditions: 1 cycle
146 of 94°C for 30s followed by 30 cycles of 94°C for 30s, 56°C for 45s and 72°C for 1min, with
147 a final extension step at 72°C for 7min. PCR products are loaded on the 2 % agarose gel and
148 stained with SYBR Safe DNA Gel Stain (Life Technologies, Carlsbad, CA USA). The primer
149 sequences have been published previously (Dijk *et al.*, 2004; Gainer *et al.*, 2011).

150

151 *Tissue collection and processing*

152 Rats were terminally anesthetized and perfusion-fixed with 4% paraformaldehyde
153 (PFA) following a heparinized saline flush, post-fixed and cryoprotected as previously
154 described (Tobin *et al.*, 2010). The eyes were enucleated and placed in 0.1M PB during the
155 heparinized saline flush before transcardial perfusion with PFA. The cornea was cut around
156 the outer edge of the iris to remove the lens and vitreous humour and the eyecups were either
157 placed in 4% PFA solution for 5 min then the retina gently removed and placed back in 4%
158 PFA for 20min or each eyecup was left in 4% PFA solution for 2h. Some retinas were fixed
159 in a solution of 4% PFA + 1% glutaraldehyde but otherwise processed as described above.
160 Tissue was then stored at 4°C in 10% sucrose, then placed in 20% sucrose solution for
161 120min and finally in 30% sucrose for 12 to 48h, until the tissues had sunk to the bottom of
162 the vials. In eyes which were required for coronal or transverse sections, the tissues were then
163 placed in Tissue-Tek CRYO-OCT (optimal cutting temperature compound) embedding
164 matrix (Fisher Scientific UK)-filled cryo-molds (Sakura Finetek UK Ltd) and gently
165 manipulated to open up and be in the appropriate orientation and then snap-frozen on
166 powdered dry ice. The retinas or eyecups were stored at -20°C until 16-µm sections were cut
167 at -15°C on a cryostat. These sections were thaw-mounted onto SupraFrost slides, allowed to
168 air-dry for 10min before being stored at -20°C until they were processed for fluorescence

169 immunocytochemistry. For retinal flat mounts, 3-4 incisions were made from the perimeter of
170 the retina almost to the centre to allow the retina to be gently flattened. The flat-mounts were
171 stored in 0.1M PB until used for immunohistochemistry. After transcardial perfusion, the
172 brains were removed and placed in a 2% PFA and 15% sucrose solution overnight and
173 transferred to 30% sucrose until the tissue had sunk. Coronal 40µm sections were cut using a
174 freezing microtome.

175

176 *Immunohistochemistry*

177 For brain sections and rat retina flat mounts, immunohistochemistry was conducted
178 using a free-floating technique. For retina sections, immunohistochemistry was conducted on
179 the slides either in slide-mailers (Fisher Scientific UK) or after the sections on each slide
180 were outlined with hydrophobic ink (ImmEdge, Vector Laboratories) and thereafter kept
181 horizontal in a light-proofed humid chamber. For each of these techniques, the sections were
182 thoroughly rinsed in 0.1M PB and incubated in 0.1M glycine in 0.1M PB for 30min at room
183 temperature. For immunohistochemistry involving exposure to a biotinylated secondary and
184 fluorescently-tagged streptavidin, sections were blocked for endogenous biotin by incubating
185 them first in 0.01% avidin in 0.1M PB for 30min, washing and then incubating in 0.001%
186 biotin in 0.1M PB for 30min. After washing, sections were incubated for 60min in a blocking
187 buffer consisting of 3-5% normal serum (matched to the host of secondary animal) + 1%
188 bovine serum albumin (BSA) + 0.1% Triton X-100 diluted in 0.1M PB. If the primary
189 antibody was raised in goat, BSA was not used in either the blocking buffer or in the
190 antibody-diluting buffer. The sections were incubated with primary antibodies (Tab. 1)
191 diluted in the blocking buffer. The primary antibodies were applied for 1-5 days at room
192 temperature for first day and thereafter at 4°C. After washing in 0.1M PB, sections were
193 incubated for 60min with secondary antibodies and then washed in 0.1M PB. Sections
194 exposed to biotinylated secondaries were then incubated for 60min with fluorescently-
195 labelled streptavidin conjugate (1:1000). Both secondary antibodies and fluorescently-
196 labelled streptavidin were diluted in 0.1M PB + 0.03% tween. After further washing, sections
197 were incubated in DAPI (4',6-diamidino-2-phenylindole, 1:33000, Life Technologies Ltd,
198 UK) for 5min at room temperature, washed and cover-slipped using either a Mowiol 4-88
199 (Calbiochem, USA) mounting medium, supplemented with 2.5% DABCO (1,4-
200 diazabicyclo[2.2.2]octane, Sigma) or Prolong Gold (Life Technologies Ltd, UK). No
201 fluorescent labelling was detected when primary antibodies were omitted or when the
202 primary antibodies (Tab. 2) were incubated with a five-fold (w/v) of control immunogen

203 before being exposed to the tissue sections (the latter control was conducted whenever a
204 control peptide was available from the supplier of that primary antibody). Most antibody
205 suppliers provided western blot analysis showing the antibody detecting protein in a single
206 band of appropriate size.

207

208 *Microscopy*

209 Fluorescence signals were acquired either using a Nikon AIR confocal or a Zeiss
210 LSM510 Axiovert confocal laser scanning microscope. In either case, the images were
211 acquired at 1024x1024 pixels, using a Nikon Plan Apochromat 1.4 NA x60 oil immersion
212 objective or a Zeiss Plan NeoFLUAR 1.4 NA x63 oil-immersion objective respectively. In all
213 cases, emissions for each fluorophore were obtained consecutively to avoid channel cross-
214 talk. Those images taken throughout each cell at Nyquist sampling rates were deconvolved
215 using Huygens software (Scientific Volume Imaging, Hilversum, Netherlands) and all images
216 were analysed using NIH ImageJ software (v1.48) and figures constructed using Microsoft
217 PowerPoint.

218

219 *Cloning of rAAV vectors and virus production*

220 In addition to tissue from transgenic rats, for morphological studies we used tissue
221 from wild-type rats given bilateral intravitreal injections (under isoflurane anesthesia) of a
222 recombinant adeno-associated virus (rAAV) which caused the expression of Venus or
223 tdTomato under the control of the vasopressin promoter. The conserved promoter region of
224 vasopressin gene, chosen using the software BLAT from UCSC ([http://genome.ucsc.edu/cgi-
225 bin/hgBlat](http://genome.ucsc.edu/cgi-bin/hgBlat)) was sub-cloned into a rAAV2 backbone carrying an ampicillin-resistance. It
226 comprises a 1.9kb sequence stretch (revealed by BLAT) that allows for cell-specific
227 expression in hypothalamic vasopressin neurons. Venus or tdTomato was introduced to the
228 plasmid as the gene of interest. Production of chimeric virions (recombinant Adeno-
229 associated virus 1/2; rAAV 1/2) was described previously (Knobloch *et al.*, 2012). Briefly,
230 human embryonic kidney cells 293 (AAV293; Agilent #240073) were calcium phosphate-
231 transfected with the recombinant AAV2 plasmid and a 3-helper system (During *et al.*, 2003).
232 rAAV genomic titers were determined with QuickTiter AAV Quantitation Kit (Cell Biolabs,
233 Inc., San Diego, California, USA) and are $\sim 10^{13}$ genomic copies per ml.

234

235 Rats were anesthetized by medetomidine/ketamine injection and placed in a tiltable
236 stereotaxic frame. A few drops of phenylephrine chlorhydrate and tropicamide (Mydrin-P®)
to induce mydriasis, oxybuprocaine chlorhydrate (Benoxil® 0.4%) for additional local

237 anaesthesia, and ofloxacin (Tarivid® 0.3%) antibiotic was administered into each eye. The
238 head was tilted with its left or right eye uppermost. Intravitreal injections were performed as
239 described by Chiu and colleagues (Chiu *et al.*, 2007). Using a very fine needle (33G,
240 Heraeus, Kulzer Japan Co., Ltd.) attached to a 0.025-ml Hamilton syringe (microliter TM
241 702), a small puncture was made in the region of the limbus and the needle was lowered into
242 the vitreous using a micromanipulator. 2-5µl of (rAAV) was intravitreally injected into both
243 eyes of transgenic or wild-type rats. The needle was left in position for 30-60s and then
244 withdrawn slowly. The procedure was repeated on the other side of the same eye before being
245 repeated on the other eye. Injections were performed under a dissecting microscope to ensure
246 correct positioning of the needle and to monitor loss of fluid from the eye. Intravitreal
247 injections were performed by a trained ophthalmologist. Virally-transfected rats were left for
248 two weeks before transcardial perfusion.

249

250 *Retrograde Tracing*

251 In 12 eGFP rats under isoflurane anesthesia, 50-100nl of the retrograde tracer (Red-
252 Retrobeads, Lumafluor Inc, Florida, USA, or Fluorogold Sigma) was microinjected
253 stereotaxically in the left SCN (bregma -1.1, lateral +0.3, depth 8.6mm from dura), IGL
254 (bregma -4.5, lateral +4.0, depth 5.5mm from dura), OPt (bregma -4.7, lateral 1.3, depth
255 4.4mm from dura) or bilaterally into the left and right superior colliculus (bregma -5.3mm,
256 lateral 1.5mm, depth 4.8mm from dura) (Paxinos & Watson, 2006) over 20 min. One week
257 later, rats were perfused transcardially with 4% PFA and brains and retinas were processed
258 for immunohistochemistry.

259

260 *Fos expression*

261 The effects of light on Fos expression on eGFP-positive RGCs and the SCN was
262 evaluated in eGFP rats fixed by transcardial perfusion during the day (noon) or night after
263 light exposure (1000 lux, for 1h, 2h before the end of the night). Standard
264 immunocytochemistry was performed on floating retinal flat mounts or SCN sections using a
265 polyclonal antibody raised in rabbit against the N-terminal amino acids 4-17 of the protein
266 product of human *c-fos* (PC38, Millipore, UK). For double immunocytochemistry, a
267 polyclonal antibody raised in chicken against eGFP (Abcam UK) was used. Antibody-antigen
268 complexes were visualized by using ABC methods with a Vector stain elite kit (Vector
269 Laboratories, Bucks, UK) intensified with nickel-intensified diaminobenzidine (Ni-DAB;
270 single immunocytochemistry) or with DAB only (double immunocytochemistry). Fos-

271 positive nuclei and the percentage of activated cells were counted in the SCN at the level of
272 maximal cross-sectional area by an observer blind to the treatment group.

273

274 *Intracerebroventricular infusion of vasopressin V1a antagonist*

275 Wild-type rats were implanted with a left lateral ventricular brain infusion cannula (Alzet
276 BIK2, Charles River Ltd, Margate, Kent, UK) under isoflurane anaesthesia via a burr hole in
277 the skull drilled 0.6mm posterior to and 1.6mm lateral to bregma (Paxinos & Watson, 2006).
278 The cannula was secured in place using dental cement glued to two stainless steel screws
279 driven into the skull and then connected via polythene tubing to a subcutaneous osmotic
280 minipump (Alzet 2001). The pumps were prepared as in instructions and filled with a
281 vasopressin V1a receptor antagonist ($d(\text{CH}_2)_5\text{Tyr}(\text{Me})^2\text{AVP}$, Dr. Manning (Kruszynski *et al.*,
282 1980)) or aCSF and set to deliver at a rate of 416 ng h^{-1} , for 3 days ($n=5-7/\text{group}$). This
283 antagonist binds similarly to V1a and V1b receptors, and the dose is about twice that used
284 previously (Subburaju & Aguilera, 2007), who delivered 230 ng h^{-1} for 28 days and showed
285 effectiveness at blocking the effects of exogenous vasopressin. Rats were housed singly and,
286 on the day of experiment, rats were moved into a brightly lit laboratory (1000 lux) and placed
287 into empty clear cages for 1h. They were then terminally anaesthetised for tissue fixation (see
288 above).

289

290

291 *In vivo* electrophysiology

292 Urethane-anaesthetised adult male wild-type rats (ethyl carbamate 1.25 g kg^{-1} , i.p.)
293 were tracheotomized and the area below the SCN was exposed using a transpharyngeal
294 approach (Ludwig *et al.*, 2002; Saeb-Parsy & Dyball, 2003). An injection cannula was placed
295 into the third ventricle (coordinates: 0.6 mm caudal to bregma, 1.5 mm lateral to midline, 5
296 mm deep) (Paxinos & Watson, 2006) for icv drug administration, and in some experiments a
297 bipolar stimulating electrode was placed onto the exposed optic nerve, as above, contralateral
298 to the recording side. Recordings were made from single cells in the SCN using a glass
299 microelectrode (tip diameter $\sim 1 \mu\text{m}$) filled with 0.9% NaCl; firing rates were recorded using
300 Spike2 software and CED 1401 interface (Cambridge Electronic Design, Cambridge, UK) on
301 a PC. The spontaneous activity of each SCN neuron was recorded for at least 5min before
302 treatment. Trains of stimuli (matched biphasic pulses; 1-ms pulses, 1mA peak-to-peak; 50Hz
303 for 0.5s, every 1min) were applied to the contralateral optic nerve. Light was applied at
304 100lux or 1500lux for 5s at 1-min intervals after the rats were held in dark conditions with

305 eyes covered with aluminum foil. Electrical or light stimulation was repeated before, during
306 and after injection of a vasopressin antagonist into the 3rd ventricle, 2-3mm caudal to the
307 recording site. The injection cannula was backfilled with vasopressin V1a antagonist (40ng in
308 2µl aCSF)(Tobin *et al.*, 2010) followed by 2µl of aCSF to prevent diffusion of antagonist into
309 the SCN; in tests, the first injection of 2µl was thus of aCSF, followed 10min later with an
310 injection of antagonist. Responses to light were averaged over 10-20 presentations; responses
311 to antagonist began ~ 5min after injection so the average of responses after this time was
312 taken. Only one cell was tested in each experiment. One of the cells tested with the antagonist
313 was not tested with aCSF; in that experiment a different cell had been tested with aCSF with
314 no response (not shown) but was lost before the antagonist could be injected.

315

316 *In vitro* electrophysiology

317 eGFP rats were terminally anesthetized with pentobarbital (50mg kg⁻¹) and retinas
318 dissected out as described previously (Schmidt & Kofuji, 2011). Retinas were treated with
319 enzymes by adding collagenase and hyaluronidase (Worthington Chemicals) to Ames'
320 solution for 10min in a 95% O₂/5% CO₂ environment, shaken gently before being washed 3
321 times in carbon-saturated Ames' solution and stored in dark for at least 1h before being moved
322 to the recording chamber. Retina flat mounts were superfused with Ames' solution (30°C–
323 32°C) at 3ml min⁻¹. Conventional whole-cell patch-clamp recordings, using a K⁺-gluconate-
324 based internal solution, were obtained as previously described (Son *et al.*, 2013). Some
325 neurons were intracellularly labeled with Alexa Fluor 555 (100µM) or biocytin (1%).
326 Recordings were obtained from eGFP-labeled VP-RGCs neurons. For bath-applied drugs,
327 mean firing activity and membrane potential values were calculated from a 2-min period
328 before drug application and in a 2-min period around the peak effect.

329

330 *Microdialysis*

331 In wild-type rats, the brain region above the SCN was exposed by the transpharyngeal
332 approach under urethane anaesthesia (ethyl carbamate 1.25g kg⁻¹, i.p.) as previously
333 described (Ludwig *et al.*, 2002). An in-house designed U-shaped microdialysis probe
334 (molecular weight cut-off of 6kDa, Fleaker[®] hollow fibre, Spectrum Medical Inc., Los
335 Angeles, CA, USA) was positioned into the left SCN after opening of the meninges. After
336 implantation, there was an equilibration period of at least 1h before six consecutive 30-min
337 dialysis samples were collected. The samples were frozen and stored at -20°C until assay for
338 vasopressin. After two 30-min baseline periods, a stimulating electrode (Clarke

339 Electromedical, SNEX-200X) placed onto the optic nerve closely behind the right eye was set
340 to deliver trains of matched biphasic pulses (0.1ms, 1mA peak-to peak; 50Hz for 5s, every
341 1min for 30min). In other experiments, light was applied (1min on/1min off for 30min) to the
342 eye contralateral to the recording site using a portable surgical light (1500lux) at early
343 morning or late evening during then third sampling period. For the early morning
344 measurements, rats were anaesthetised at ZT0, and kept in the dark (covering the eyes with
345 aluminum foil) before stimulating with light at ZT4. For the late evening measurements, rats
346 were anaesthetised at ZT9 and then kept in the dark (covering the eyes with aluminum foil)
347 before stimulating with light at ZT12. The SCN was dialysed with aCSF (pH 7.2,
348 composition in mM: NaCl 138, KCl 3.36, NaHCO₃ 9.52, Na₂HPO₄ 0.49, urea 2.16, CaCl₂
349 1.26, MgCl₂ 1.18) at 3µl min⁻¹). At the end of each experiment, during sample period six, a
350 modified aCSF containing 150mM KCl plus 100µM veratridine was retrodialysed into the
351 SCN to trigger vasopressin release as a control for probe placement, and only data from
352 experiments in which this evoked at least a 3-fold increase in vasopressin concentration were
353 analysed. Brains were removed and cut for histological confirmation of microdialysis probe
354 placement.

355 Vasopressin in microdialysates was measured after lyophilization as previously
356 described (Landgraf *et al.*, 1995; Paiva *et al.*, 2016) by a sensitive and selective
357 radioimmunoassay (RIA; detection limit: 0.1pg sample⁻¹; cross-reactivity less than 0.7%,
358 RIAGnosis, Sinzing, Germany). Samples for measurement were blind coded.

359

360 *Statistics*

361 *Fos expression in the retina.* Three groups were compared by the non-parametric Kruskal-
362 Wallis test, followed by Mann-Whitney U tests to test the hypotheses a) that light activates
363 Fos expression in VP-RGCs and b) that expression is higher in the light than in the dark
364 period.

365 *Retinal vasopressin content.* Two groups (n=7) were compared to test the hypothesis that the
366 vasopressin content of the retina differs between dark and night. Values were compared by a
367 two-tailed t-test.

368 *Fos expression in the SCN.* First, we compared light-induced Fos expression in early vs late
369 night. In subsequent experiments we tested the hypothesis that a V1a antagonist would
370 attenuate light-induced Fos expression in the late night. Fos-positive nuclei were counted in
371 each SCN in 3-5 sections per rat, and the median calculated; to combine these for group
372 values, the medians were log-transformed as their distributions were skewed; n values are

373 animal means. Groups were compared with a one-tailed t-test, as this experiment tested a
374 predetermined unidirectional hypothesis.

375 *Microdialysis*. In the experiment shown in Fig. 6, the basal levels of vasopressin varied in a
376 3-fold range between experiments, and so all data were normalized to the concentration in the
377 first basal sample. The normalized data (excluding the first basal sample) from the two
378 groups were compared by a repeated measures ANOVA followed by pairwise tests, using
379 Bonferroni's and Tukey's multiple comparisons test.

380 *In vivo electrophysiology*. Two hypotheses were tested in separate experiments: that V1a
381 antagonist attenuates SCN responses to light, and that it attenuates SCN responses to
382 electrical stimulation of the optic nerve. Each of these was tested by a paired comparison of
383 the (mean) response in control condition and the mean response after application of the
384 antagonist, using a two-tailed Wilcoxon signed rank test.

385

386

387 **Results**

388 *Characterisation of VP-RGCs*

389 Vasopressin content in the retina has been previously described, and vasopressin has been
390 found (by immunocytochemistry) to be expressed in some cells in both the ganglion cell layer
391 and the inner nuclear layer of the retina (Gauquelin et al., 1983; Djeridane, 1994; Moritoh et
392 al., 2011). We studied these cells in a transgenic rat strain in which eGFP (enhanced green
393 fluorescent protein) is expressed under the control of the vasopressin promoter (Fig. 1A,B)
394 (Ueta et al., 2005). eGFP-expressing cells comprised about 1% of cells in the ganglion cell
395 layer ($1.07 \pm 0.01\%$ of 33868 cells from 9 retinas), and were sparsely distributed across the
396 whole retina. By immunocytochemistry, we established that all the eGFP-expressing cells
397 that we examined in the retina also expressed vasopressin-associated neurophysin: this large
398 peptide is part of the vasopressin precursor peptide (Fig. 1C). eGFP (and vasopressin
399 neurophysin) was also expressed in some small cells in the inner nuclear layer, which
400 contains interneurons that do not project out of the retina.

401 The VP-RGCs were heterogeneous in size. In the inner nuclear layer, most e-GFP
402 expressing cells were small: a sample of 21 of these cells had a mean (S.E.M.) cross-sectional
403 area of $58 \pm 2.6 \mu\text{m}^2$ (range 48-85 μm^2). By contrast, in a sample of 43 eGFP-expressing cells
404 in the ganglion cell layer, 25 small cells had a mean (S.E.M.) cross-sectional area of
405 $83 \pm 2.7 \mu\text{m}^2$ (range 62-99 μm^2), while the ten largest cells had a mean (S.E.M.) cross-sectional
406 area of $291 \pm 13.2 \mu\text{m}^2$ (range 154-333 μm^2). Using triple immunohistochemistry, we found

407 that many large (but not small) VP-RGCs co-expressed the vesicle glutamate transporter 2
408 (vGLUT-2), indicating that these cells use glutamate as a neurotransmitter (Fig. 1E)
409 (Fujiyama *et al.*, 2003). In mammals, melanopsin is found in intrinsically photosensitive
410 RGCs that project to the SCN and plays a critical role in regulating circadian rhythms
411 (Provencio *et al.*, 2000; Hattar *et al.*, 2002; Hankins *et al.*, 2008). VP-RGCs were often
412 closely juxtaposed to immunoreactive melanopsin cells (Fig. 1F). Of the small VP-RGCs,
413 only one cell of 300 counted contained detectable immunoreactive melanopsin, but, of the
414 large VP-RGCs, 25% (21/80) co-expressed melanopsin. We found no co-localisation of
415 eGFP with calretinin, parvalbumin, tyrosine hydroxylase, glycine, choline acetyltransferase
416 or GAD65/67 (Fig. 2A-F), which label known subpopulations of retinal interneurons (Marc
417 & Jones, 2002).

418 The vasopressin-eGFP transgene encodes a modified vasopressin precursor with
419 eGFP fused in-frame at the C terminus (Ueta *et al.*, 2005 and D. Murphy, personal
420 communication). The signal peptide, vasopressin and neurophysin portions of the precursor
421 are intact, and may be expressed from the transgene, thus the vasopressin-associated
422 neurophysin in eGFP rats may reflect either endogenous expression or transgene-driven
423 expression. We therefore confirmed the expression of vasopressin in retinal cells in wild-type
424 rats using antibodies against vasopressin-neurophysin (see below), the presence of
425 vasopressin mRNA in the retina by PCR (Fig. 1D, 3B), and the production of vasopressin by
426 radioimmunoassay. The vasopressin content of the retina in wild-type rats was higher in the
427 late afternoon (ZT11) than in the early morning (ZT1; 25 ± 2.6 vs. 52 ± 8 pg per retina, $n=7$ per
428 group, $P < 0.015$), consistent with light-induced activation of synthesis.

429

430 *Venus labelling*

431 To visualise the axons of the VP-RGCs in wild-type rats, we made intravitreal
432 injections of a recombinant adeno-associated virus (rAAV) that results in the expression of a
433 fluorescent protein Venus (Figs. 3A,B; supplementary animation) or tdTomato under the
434 control of 1.9 kbp of the vasopressin promoter (Fig. 4). We confirmed the successful
435 transfection of retinal vasopressin cells by immunohistochemistry (Fig. 3B) for vasopressin
436 neurophysin. This confirms that the large RGCs do indeed express the endogenous
437 vasopressin gene, as the AAV vector does not contain vasopressin coding sequences.

438 Unlike the eGFP-vasopressin transgenic rats, where the eGFP is packaged inside the
439 same vesicles as vasopressin (Ueta *et al.*, 2005), these fluorescent proteins are released into
440 (and fill) the cytoplasm of the neurons allowing tracking of thin neurites (Knobloch *et al.*,

441 2012). In the transfected retinas, we found Venus labelling in the ganglion cell layer but not
442 in the inner nuclear layer (Fig. 3C,D). Only larger VP-RGCs expressed Venus; no Venus was
443 found in the small cells in either the inner nuclear layer or the ganglion cell layer. In three
444 retinas we sampled 220 Venus-labelled cells and 113 melanopsin-labelled cells; 45% of the
445 Venus-labelled cells contained immunoreactive melanopsin and 88% of the melanopsin cells
446 contained Venus, suggesting that most melanopsin-containing cells express vasopressin. We
447 traced the passage of Venus-labelled axons into the optic nerve (Fig. 3E), and found a dense
448 plexus in the ventrolateral SCN (Fig. 3F). Using triple immunohistochemistry for Venus,
449 vGLUT-2 and vasoactive intestinal polypeptide (VIP) or gastrin-releasing peptide (GRP) we
450 found that 74% of VIP cells and 66% of GRP cells were apposed by boutons from Venus-
451 labelled fibres (Fig. 3I,J). The Venus-labelled fibres co-expressed vGLUT-2 indicating that
452 they were glutamatergic; as expected, vGLUT-2 was not co-expressed with either VIP or
453 GRP, which are both known to use GABA as a conventional neurotransmitter (Belenky *et al.*,
454 2008).

455 We also found Venus-labelled fibres in the intergeniculate leaflet (IGL), which is
456 involved in regulation of circadian rhythms via its projections to the SCN (Hattar *et al.*,
457 2006), and in the olivary pretectal nucleus (OPt), which controls the pupillary light reflex
458 (Gamlin, 2006). However, we found no Venus-labelled fibres entering the superior colliculus,
459 which is a major projection area of classical image-forming RGCs (Feinberg & Meister,
460 2015) (Fig. 4), some were found on the outskirts of the superior colliculus, but none were
461 seen to enter this region. In two animals we transfected the right eye with AAV expressing
462 Venus and the left eye with an AAV expressing tdTomato, both under the control of the
463 vasopressin promoter. The labeled fibers terminated in the SCN, IGL and OPt (Fig. 4); most
464 fibers were found at sites contralateral to the injected eye, but there was a substantial
465 ipsilateral projection to the SCN in particular.

466

467 *Retrograde tracing*

468 We confirmed these projections by retrograde tracing studies (Fig. 3G,H). When
469 retrograde tracer beads were injected into the SCN, IGL or OPt (n=2-4 per area) we found
470 labelling of large (but not small) eGFP-positive cells in the ganglion cell layer, and no
471 labelling of any cells in the inner nuclear layer. We found no labelling after injections into the
472 superior colliculus (Fig. 3H). To estimate how many of the RGCs that project to the SCN
473 express vasopressin, we injected fluorogold into the SCN to fill this region completely (Fig.
474 3G). For the injection which achieved the best fill, we studied seven retinal sections with

475 confocal microscopy. Of 176 melanopsin-labelled cells, 142 were retrogradely labelled with
476 fluorogold; of these, 41 also expressed eGFP. In the same sections, we found only 8 VP-
477 RGCs that were labeled with fluorogold but which appeared to contain no melanopsin. These
478 experiments confirmed that most of the retinal cells that project to the SCN contain
479 immunoreactive melanopsin, and that vasopressin is expressed in a substantial subset of these
480 cells and also in some cells that project to the SCN which did not apparently contain
481 detectable amounts of immunoreactive melanopsin.

482

483 *Light responsiveness of RGCs*

484 To determine the response of VP-RGCs to light we measured the expression of the
485 immediate early gene *c-fos* in the retina by immunocytochemical detection of Fos, the protein
486 product of *c-fos*. In response to 1-h light stimulation of dark-adapted retinas (ZT21), there
487 was a significant increase in Fos expression in VP-RGCs ($8.1\pm 1.0\%$ of VP-RGC's expressed
488 Fos after light exposure vs. $0.2\pm 0.2\%$ with no light exposure, $n=3$ and $n=6$ respectively,
489 $p=0.0019$, Fig. 5A,B). Fos expression in VP-RGCs was even higher in retinas taken at ZT6
490 ($13.8\pm 3.8\%$, $n=6$), suggesting sustained expression of Fos in VP-RGCs throughout the day.

491 To characterise the responsiveness of VP-RGCs to light, we made *in vitro* patch-
492 clamp recordings from 88 large RGCs identified by their expression of e-GFP; 58 of these
493 cells were transiently excited by light, and the other 30 were inhibited (Fig. 5C,D);
494 previously, all immunoreactive melanopsin RGCs have been reported to be excited by light
495 (Schmidt *et al.*, 2011). Current-clamp and voltage-clamp recordings from the light-activated
496 VP-RGCs showed that afferent synaptic activity was increased during light stimulation,
497 suggesting that activation was mediated at least partially by synaptic input (Fig. 5F). The
498 close juxtaposition of the VP-RGCs to melanopsin cells indicates that they may receive these
499 excitatory synaptic inputs from neighboring, intrinsically photosensitive melanopsin cells
500 (Schmidt *et al.*, 2011; Hughes *et al.*, 2016).

501

502 *Vasopressin actions in the SCN*

503 We then recorded the spike activity of single SCN neurons in urethane-anesthetised
504 rats (Tsuji *et al.*, 2016). About two thirds of light-responsive cells (150/222) were excited by
505 light (5-s pulses) and about one third were inhibited. In ten cells excited by light (each from a
506 different rat), responses were measured before and after injection of aCSF and after injection
507 of a vasopressin V1a receptor antagonist into the third ventricle. The light-induced activation
508 was unaffected by aCSF injection but was reduced by $30\pm 8\%$ after antagonist injection

509 (Wilcoxon matched pairs signed rank test; $P=0.004$; Fig. 6F). We also tested the responses of
510 SCN neurons to electrical stimulation of the retino-hypothalamic tract (RHT; 5-s trains at
511 50Hz) (Fig. 6A-E). Seven SCN neurons (from seven rats) showed a prolonged excitatory
512 response (for 3-7s after stimulation) that was attenuated by icv injection of the V1a antagonist
513 (Fig. 6E).

514 A short light pulse, given during the subjective night, induces Fos expression in the
515 SCN, and this correlates with the ability of light to phase-shift activity-rest cycles (Fig. 7)
516 (Ding *et al.*, 1994). Consistent with previous studies, 60-min of light exposure at Z21 induced
517 robust Fos expression in the SCN, and this activation was significantly greater than that
518 induced by the same light exposure given at ZT15 (Fig. 7B). In separate experiments, rats
519 were chronically infused icv with the V1a antagonist or vehicle via a sub-cutaneously
520 implanted osmotic minipump connected to a cannula implanted in the lateral cerebral
521 ventricle. Light-induced Fos expression at Z21 was significantly less in rats infused with the
522 V1a antagonist (Fig. 7A,C) than in vehicle-infused rats.

523 Finally, we measured vasopressin release in the SCN (by microdialysis in urethane-
524 anaesthetised rats) in response to light exposure. In pilot experiments we found that
525 application of light (1 min on, 1 min off for 40 min) to the contralateral eye at ZT6 increased
526 vasopressin release in the SCN from 0.54 ± 0.14 to 1.76 ± 0.35 pg sample⁻¹ in samples collected
527 every 40 min ($n=6$ per group, $p<0.05$). In two further groups of rats, we collected 30-min
528 samples at the beginning and end of subjective day in before and after light was given for 30
529 min. The ‘early morning’ group was exposed to light at ZT3 after being maintained in the
530 dark continuously after the preceding dark phase; the ‘evening’ group was exposed to light at
531 ZT12 after being maintained in the dark from ZT9, to ensure dark adaptation of light
532 responsiveness. In the ‘early morning’ group, light exposure was followed by a significant
533 increase in vasopressin concentration, whereas in the ‘late evening’ group, light exposure
534 produced a significant decrease (Fig. 7D).

535

536 **Discussion**

537 The present study shows that vasopressin, well known to be an important output of
538 the SCN (Kalsbeek *et al.*, 2010), is also a time-dependent mediator of light information from
539 the retina to the SCN, and so is likely to contribute to the effects of vasopressin on jet-lag
540 (Yamaguchi *et al.*, 2013). The expression of neuropeptides in this projection has clear
541 functional significance. These cells use glutamate as a neurotransmitter, secreted from small
542 synaptic vesicles. Because glutamate can be rapidly recycled, this signalling is constantly

543 available. However, many of the RGCs that project to the SCN also contain the neuropeptide
544 PACAP (Hattar *et al.*, 2002; Schmidt *et al.*, 2011), or as described here, vasopressin. At
545 present, we do not know whether vasopressin and PACAP are co-expressed or are in separate
546 populations of RGCs. Neuropeptides are not contained in the same vesicles as glutamate, but
547 are packaged in separate, large vesicles that are synthesised at the cell body and transported
548 along the axons (Burbach *et al.*, 2001): these vesicles cannot be recycled as small synaptic
549 vesicles are. Light stimulation rapidly induces Fos expression in VP-RGCs, and induction of
550 Fos expression is implicated in the regulation of neuronal vasopressin synthesis (Cunningham
551 *et al.*, 2004). Thus, it is likely that, in VP-RGCs, Fos expression is linked to up-regulation of
552 peptide synthesis to replenish what has been released from the terminals. However, the path
553 length from retina to SCN in the rat is >20mm, and (in magnocellular vasopressin neurons)
554 vasopressin-containing vesicles are transported along axons at only ~140mm/day (Burbach *et al.*,
555 2001). Given this, and given the delays between stimulation and production of new
556 vesicles, the depletion of peptide by light-induced activation of release in the SCN cannot be
557 replenished without a lag time of several hours. Thus, at the terminals in the SCN, the
558 availability of peptide for release must be subject to a diurnal cycle of depletion and
559 replenishment.

560 We have shown here that light given at the end of the dark phase consistently evokes
561 measurable vasopressin release in the SCN, whereas light given at the beginning of the dark
562 phase does not. We predicted that light stimulation would increase vasopressin release from
563 retinal afferents, and would excite a majority of the first order recipient neurons in the SCN.
564 The retinal afferents do innervate predominantly VIP and GRP neurons, but not directly
565 innervate the intrinsic vasopressin cells of the SCN, which are regulated by inhibitory
566 GABAergic projections by the retinal recipient neurons. However, some of the retinal
567 recipient neurons are inhibited by light, so there may be activation of intrinsic vasopressin
568 cells from these inputs. In addition, it has been suggested that GABA may excite some SCN
569 vasopressin neurons (Belenky *et al.*, 2010). Thus, how much of the vasopressin collected in
570 the microdialysates is released from the retina projection or released from the endogenous
571 population of SCN vasopressin neurons in response to light stimulation is unclear. SCN
572 vasopressin neurons project to the paraventricular nucleus of the hypothalamus, the
573 subparaventricular zone, medial preoptic area, and into the contralateral SCN. SCN
574 vasopressin neurons have also axon collaterals which remain inside the boundaries of the
575 SCN (Pennartz *et al.*, 1998) and release vasopressin from their somata and dendrites (Castel
576 *et al.*, 1996).

577 We have also shown that light-induced Fos expression in the SCN is higher at the end
578 of the night than earlier, and SCN Fos expression has been linked to light-induced phase
579 shifts. Accordingly, cyclical availability of neuropeptides for release may explain why a light
580 pulse given close to the end of the night is more likely to result in a phase advance of
581 circadian rhythms than one given earlier.

582 Exactly why light is so ineffective at eliciting Fos expression in the early part of the
583 dark phase remains intriguing; even if the retinal terminals are depleted of vasopressin they
584 should still be releasing glutamate in response to light. The answer may simply be that,
585 although c-fos is often thought of as an indiscriminate marker of neuronal excitation, this is
586 over-simplistic: in magnocellular oxytocin neurons for example, the neuropeptide α -MSH
587 induces Fos expression but inhibits neuronal activity (Sabatier *et al.*, 2003), while antidromic
588 stimulation of increased spike activity is completely ineffective at increasing Fos expression
589 (Luckman *et al.*, 1994). The likely mechanistic link between synaptic activation appears to be
590 via increased intracellular calcium, and as vasopressin is a potent mobiliser of intracellular
591 calcium stores (Sabatier *et al.*, 1998), it may be a particularly potent inducer of Fos
592 expression.

593 Vasopressin is involved in diverse physiological and behavioural processes;
594 vasopressin secreted from the pituitary gland is essential for fluid and electrolyte balance, but
595 vasopressin released within the brain has many roles, including in social behaviour,
596 aggression, and in behavioural rhythms. Vasopressin is an important output of the SCN; its
597 secretion into the CSF peaks in the early morning and declines by late afternoon (Kalsbeek *et al.*,
598 2010), and its targets include vasopressin cells in other parts of the hypothalamus. In
599 particular, vasopressin released from the SCN during late sleep activates osmosensory
600 afferents to the vasopressin neurons in the supraoptic nucleus (Trudel & Bourque, 2010) and
601 to neurons in the organum vasculosum of the lamina terminalis (Gizowski *et al.*, 2016).
602 Supraoptic neurons secrete vasopressin from nerve terminals in the posterior pituitary which
603 acts on the kidneys to concentrate the urine. Regulation of this antidiuretic system by the
604 SCN suppresses nocturnal enuresis, and is important in maintaining sleep. Magnocellular
605 vasopressin neurones of the supraoptic nucleus also directly control a diversity of behavioural
606 processes, via central axonal projections and via extensive dendritic secretion of vasopressin
607 (Ludwig & Leng, 2006; Neumann & Landgraf, 2012; Stoop, 2012). Thus although
608 vasopressin is expressed at several sites in the nervous system as well as in the retina, it
609 appears that some of these vasopressin neurons are linked in functionally coherent chains to
610 integrate multiple physiological and behavioural functions.

611 Shift work that includes a night-time rotation and long distance travel has become an
612 unavoidable attribute of today's 24-h society. The related disruption of the human circadian
613 time organization leads in the short-term to an array of jet-lag-like symptoms, and in the
614 long-run it contributes to weight gain and obesity, metabolic syndrome, type II diabetes, and
615 cardiovascular disease. Studies suggest increased cancer risk, symptoms of insomnia,
616 depression, elevated cortisol levels, cognitive impairment, and premature mortality (Hastings
617 *et al.*, 2003; Froy, 2011; Kondratova & Kondratov, 2012). The mechanisms leading to
618 circadian dysfunction are largely unknown. The reported association of vasopressin with jet-
619 lag (Yamaguchi *et al.*, 2013) raises the interesting possibility that interventions in vasopressin
620 signalling from the retina may have important therapeutic benefits.

621
622

623

624 **Figure Legends**

625 **Figure 1: Vasopressin neurons in the retina.**

626 **A**, Flat mount of retina, focused on the ganglion cell layer (GCL), shows dispersed eGFP-expressing
627 cells (green cells); the blue staining is a nuclear marker DAPI, to show the location of all cells in the
628 field of view; the inset shows the location of the image within the flat mount. **B**, eGFP-cells occur in
629 both the ganglion cell layer (GCL) and the inner nuclear layer (INL), as shown in a cross section of
630 the flat mount. **C**, eGFP-cells express vasopressin-neurophysin (VP-NP); the successive images show
631 fluorescence for eGFP, immunoreactive VP-NP, and overlaid images. **D**, PCR confirmation of
632 expression of vasopressin mRNA (VP, 77bp) and actin mRNA in the supraoptic nucleus (positive
633 control) and the retina of wild type rats; the supraoptic nucleus contains magnocellular neurons that
634 project to the posterior pituitary gland. Note there is no detectable oxytocin mRNA (OXT, 62bp) in
635 the retina; oxytocin is a closely related peptide that is also expressed in the supraoptic nucleus. **E**,
636 eGFP-cells (shown in a flat mount) co-express the vesicle glutamate transporter vGLUT-2 (white
637 arrows) indicating that they use glutamate as a conventional neurotransmitter. **F**, Some eGFP-cells co-
638 express the photopigment melanopsin (white arrows, yellow arrow shows a cell immunopositive for
639 melanopsin only).

640

641 **Figure 2: Vasopressin neurons in the retina.**

642 Immunohistochemistry for retinal cell types Fluorescence immunohistochemistry showing that eGFP-
643 expressing RGCs (green in top layer) and amacrine cells (green lower layer) do not co-express
644 markers commonly used to identify retinal cells (red), including calcium binding proteins (**A-C**),
645 neuropeptides (**D-F**), and “classical” transmitters (**G-J**).

646

647 **Figure 3: VP-RGC transfection and projections.**

648 **A**, Scheme of the viral vector used to infect VP-RGCs. **B**, Intravitreal injection in wild type rats of a
649 rAAV-expressing Venus (green) under the control of the vasopressin promoter infects RGCs that
650 express vasopressin neurophysin (VP-NP, red; yellow in overlay). **C**, Venus labelling in a retinal flat
651 mount. **D**, dendrites of RGCs branching into the inner nuclear layer (INL) (**D**) or ganglion cell layer
652 (GCL) (**Di**). **E**, Venus-labelled axonal projections converge on the optic disc, where the optic nerve
653 leaves the retina. **F**, enlarged in **Fi**, The VP-RGCs project (green fibres; Venus) to the ventrolateral
654 SCN; intrinsic vasopressin cells in red. **G,H**, Retrograde tracer is found in some VP-RGCs (**Gi,Hi**)
655 after microinjection into the SCN (**G**) (fluorogold), but not after injection into the superior colliculus
656 (**H**, Fluoro-Red beads). **I,J**, Terminal boutons of Venus-labelled fibres in the SCN express vGLUT-2
657 and target (**I**) vasoactive intestinal polypeptide (VIP) and (**J**) gastrin-releasing peptide (GRP) cells.
658 The blue staining is a nuclear marker DAPI. 3V 3rd ventricle, OC optic chiasm; ITR inverted terminal
659 repeat sequence.

660

661 **Figure 4: Projections of VP-RGCs**

662 DAB immunohistochemistry in wild type rats after intravitreal injection of a rAAV-expressing Venus
663 under the control of the vasopressin promoter into the retina shows some fibers projecting to the (**A**)
664 intergeniculate leaflet and (**B**) olivary pretectal nucleus, but not to the (**C**) superior colliculus. **D**,
665 Scheme of the viral vectors used to infect VP-RGCs. Intravitreal injection of a rAAV-expressing
666 Venus (green) into (**E**) the right retina and tdTomato (red) into (**F**) the left retina shows (**G-K**) that the
667 fibers terminate in the SCN, intergeniculate leaflet (IGL) and olivary pretectal nucleus (OPt) with the
668 majority contralateral to the injected eye.

669

670 **Figure 5: Light exposure excites VP-RGCs.**

671 **A**, The expression of Fos in VP-RGCs in the day (ZT6). **B**, Expression is higher in the day (ZT6) than
672 in the dark (ZT21) and is induced by light stimulation in the dark (*mean difference 7.5, 95% CI 4.0 to*
673 *11.0, **P=0.0019*). Patch-clamp recordings of VP-RGCs showing examples of (**C**) a transient increase
674 in spike activity during light exposure, and (**D**) inhibition of spike activity. **E**, Example of a patch-
675 clamp recorded eGFP-labeled RGC filled with biocytin (red; overlay with green gives the yellow
676 signal in the soma). **F**, spikes in response to light are initiated by excitatory postsynaptic potentials
677 (arrow). **G**, Summary of electrophysiology data showing changes in voltage potential (Vm, for
678 stimulated (*mean difference 16.2, 95% CI 12.8 to 19.6, ***P=0.0001*) and inhibited neurons (*mean*
679 *difference -6.56, 95% CI -7.9 to -5.2, ***P=0.0001*), n=58 excited cells, 30 inhibited cells, means +
680 S.E.M; *** P<0,001).

681 [Figure 5B source data](#); [Figure 5G source data](#)

682

683 **Figure 6: Vasopressin effects on SCN cells.**

684 **A,B,** Icv injection of a vasopressin V1a antagonist blocks the response of an SCN neuron *in vivo* to
685 electrical stimulation of the RHT (grey bar), shown in post-stimulus time histograms before (**A**) and
686 after (**B**) antagonist injection. **C,** Example of the response of a SCN cell to repeated electrical
687 stimulation of the RHT; the black symbols plot the number of spikes recorded in the 6s after
688 stimulation of the RHT for 0.5s at 50Hz delivered every minute; the open symbols plot the number of
689 spikes in the following 6s. A V1a antagonist given icv (arrow) markedly attenuates the response to
690 stimulation for about 20 min after a lag of 3 min. **D,** Mean (S.E.M.) response to RHT stimulation of
691 the same cell, shown in blue for the first ten responses plotted in **C** and in red for the ten responses
692 plotted between 20 and 30 min in **C**. **E,** Mean responses to RHT stimulation of 7 SCN cells plotted as
693 % differences to control firing rate after icv injection of aCSF followed by icv injection of the V1a
694 antagonist and after recovery (washout) (** $P=0.009$ vs. control; two-tailed Wilcoxon signed rank
695 test; numbers in columns are n/group). **F,** Icv injection of antagonist attenuates the responses of SCN
696 neuron *in vivo* to light: this panel shows the response of a representative SCN neuron to light; it shows
697 the mean (S.E.M.) responses to repeated light exposures before and after injection of the antagonist
698 (n=9 in each case).

699 [Figure 6E source data.xlsx](#); [Figure 6F source data.xlsx](#)

700

701 **Figure 7: Vasopressin effects on SCN Fos expression.**

702 **A,** Hypothalamic sections at the level of the SCN stained for Fos (black nuclear stain), and lightly
703 counterstained with nuclear fast red. A 60-min light pulse presented at the beginning of the dark
704 period (ZT15) induces more Fos expression in the SCN than a pulse presented towards the end of the
705 dark period (ZT21). Light-induced Fos expression is attenuated by a vasopressin V1a antagonist. **B,**
706 Data (median numbers of Fos cells counted per SCN section) from all individual animals are given as
707 points (*mean difference 0.39, 95%CI 0.1 to 0.68, ** $P=0.0095$*). **C,** Data (median numbers of Fos cells
708 counted per SCN section) from all individual animals are given as points (*mean difference 0.54,*
709 *95%CI -1.1 to 0.02, ** $P=0.029$*). **D,** Light stimulation increases the vasopressin content in SCN
710 microdialysates in the ‘early morning’ group (light exposure at ZT3) but not the ‘evening’ group
711 (light at ZT12) as measured by radioimmunoassay (RM ANOVA followed by Bonferroni’s and
712 Tukey’s multiple comparisons tests). *Mean difference 0.54, 95%CI 0.23 to 0.85, *** $P=0.0001$; mean*
713 *difference 0.41, 95%CI 0.1 to 0.72, ** $P=0.005$; mean difference -0.47, 95%CI -0.75 to -0.18,*
714 *+++ $P=0.0006$.* Bars show means+S.E.M. Numbers in columns are n per group.

715 [Figure 7B source data.xlsx](#); [Figure 7C source data.xlsx](#); [Figure 7D source data.xlsx](#)

716

717 **Table 1. Primary Antibodies used for retina and SCN immunohistochemistry**

718

719 **Table 2. Secondary and visualisation reagents used for retina and SCN**

720

721 **Supplementary animation:**

722 Animation of confocal images, showing cumulative stacking of sequential z slices from a
723 retina flat mount, providing a 3D representation of the dendritic arborization of Venus filled
724 (green) vasopressin expressing retinal ganglion cells.

725

726 **References**

727

728 Albrecht U. (2012). Timing to perfection: the biology of central and peripheral circadian
729 clocks. *Neuron* **74**, 246-260.

730

731 Antle MC, Smith VM, Sterniczuk R, Yamakawa GR & Rakai BD. (2009). Physiological
732 responses of the circadian clock to acute light exposure at night. *Rev Endocr Metab*
733 *Disord* **10**, 279-291.

734

735 Belenky MA, Sollars PJ, Mount DB, Alper SL, Yarom Y & Pickard GE. (2010). Cell-type
736 specific distribution of chloride transporters in the rat suprachiasmatic nucleus.
737 *Neuroscience* **165**, 1519-1537.

738

739 Belenky MA, Yarom Y & Pickard GE. (2008). Heterogeneous expression of gamma-
740 aminobutyric acid and gamma-aminobutyric acid-associated receptors and
741 transporters in the rat suprachiasmatic nucleus. *J Comp Neurol* **506**, 708-732.

742

743 Berson DM, Dunn FA & Takao M. (2002). Phototransduction by retinal ganglion cells that
744 set the circadian clock. *Science* **295**, 1070-1073.

745

746 Bielsky IF, Hu SB, Ren X, Terwilliger EF & Young LJ. (2005). The V1a vasopressin
747 receptor is necessary and sufficient for normal social recognition: a gene replacement
748 study. *Neuron* **47**, 503-513.

749

750 Burbach JP, Luckman SM, Murphy D & Gainer H. (2001). Gene regulation in the
751 magnocellular hypothalamo-neurohypophysial system. *Physiol Rev* **81**, 1197-1267.

752

753 Castel M, Morris J & Belenky M. (1996). Non-synaptic and dendritic exocytosis from dense-
754 cored vesicles in the suprachiasmatic nucleus. *Neuroreport* **7**, 543-547.

755

756 Chiu K, Chang RC & So KF. (2007). Intravitreal injection for establishing ocular diseases
757 model. *JoVE*, 313.

758

759 Cunningham JT, Penny ML & Murphy D. (2004). Cardiovascular regulation of supraoptic
760 neurons in the rat: synaptic inputs and cellular signals. *Prog Biophys Mol Biol* **84**,
761 183-196.

762

763 Dijk F, Kraal-Muller E & Kamphuis W. (2004). Ischemia-induced changes of AMPA-type
764 glutamate receptor subunit expression pattern in the rat retina: a real-time quantitative
765 PCR study. *Invest Ophthalmol Vis Sci* **45**, 330-341.
766

767 Ding JM, Chen D, Weber ET, Faiman LE, Rea MA & Gillette MU. (1994). Resetting the
768 biological clock: mediation of nocturnal circadian shifts by glutamate and NO.
769 *Science* **266**, 1713-1717.
770

771 Djeridane Y. (1994). Immunohistochemical evidence for the presence of vasopressin in the
772 rat harderian gland, retina and lacrimal gland. *Exp Eye Res* **59**, 117-120.
773

774 Donaldson ZR & Young LJ. (2008). Oxytocin, vasopressin, and the neurogenetics of
775 sociality. *Science* **322**, 900-904.
776

777 During MJ, Young D, Baer K, Lawlor P & Klugmann M. (2003). Development and
778 optimization of adeno-associated virus vector transfer into the central nervous system.
779 *Methods Mol Med* **76**, 221-236.
780

781 Feinberg EH & Meister M. (2015). Orientation columns in the mouse superior colliculus.
782 *Nature* **519**, 229-232.
783

784 Froy O. (2011). Circadian rhythms, aging, and life span in mammals. *Physiology (Bethesda)*
785 **26**, 225-235.
786

787 Fujiyama F, Hioki H, Tomioka R, Taki K, Tamamaki N, Nomura S, Okamoto K & Kaneko
788 T. (2003). Changes of immunocytochemical localization of vesicular glutamate
789 transporters in the rat visual system after the retinofugal denervation. *J Comp Neurol*
790 **465**, 234-249.
791

792 Gainer H, Ponzio TA, Yue C & Kawasaki M. (2011). Intron-specific neuropeptide probes.
793 *Methods Mol Biol* **789**, 89-110.
794

795 Gamlin PD. (2006). The pretectum: connections and oculomotor-related roles. *Prog Brain*
796 *Res* **151**, 379-405.
797

798 Gauquelin G, Geelen G, Louis F, Allevard AM, Meunier C, Cuisinaud G, Benjanet S, Seidah
799 NG, Chretien M, Legros JJ & et al. (1983). Presence of vasopressin, oxytocin and
800 neurophysin in the retina of mammals, effect of light and darkness, comparison with
801 the neuropeptide content of the neurohypophysis and the pineal gland. *Peptides* **4**,
802 509-515.
803

804 Gizowski C, Zaelzer C & Bourque CW. (2016). Clock-driven vasopressin neurotransmission
805 mediates anticipatory thirst prior to sleep. *Nature* **537**, 685-688.
806

807 Golombek DA & Rosenstein RE. (2010). Physiology of circadian entrainment. *Physiol Rev*
808 **90**, 1063-1102.
809

810 Hankins MW, Peirson SN & Foster RG. (2008). Melanopsin: an exciting photopigment.
811 *Trends Neurosci* **31**, 27-36.
812

- 813 Hastings MH, Reddy AB & Maywood ES. (2003). A clockwork web: circadian timing in
814 brain and periphery, in health and disease. *Nat Rev Neurosci* **4**, 649-661.
815
- 816 Hattar S, Kumar M, Park A, Tong P, Tung J, Yau KW & Berson DM. (2006). Central
817 projections of melanopsin-expressing retinal ganglion cells in the mouse. *J Comp*
818 *Neurol* **497**, 326-349.
819
- 820 Hattar S, Liao HW, Takao M, Berson DM & Yau KW. (2002). Melanopsin-containing retinal
821 ganglion cells: architecture, projections, and intrinsic photosensitivity. *Science* **295**,
822 1065-1070.
823
- 824 Hughes S, Jagannath A, Rodgers J, Hankins MW, Peirson SN & Foster RG. (2016).
825 Signalling by melanopsin (OPN4) expressing photosensitive retinal ganglion cells.
826 *Eye (Lond)* **30**, 247-254.
827
- 828 Kalsbeek A, Fliers E, Hofman MA, Swaab DF & Buijs RM. (2010). Vasopressin and the
829 output of the hypothalamic biological clock. *J Neuroendocrinol* **22**, 362-372.
830
- 831 Knobloch HS, Charlet A, Hoffmann LC, Eliava M, Khrulev S, Cetin AH, Osten P, Schwarz
832 MK, Seeburg PH, Stoop R & Grinevich V. (2012). Evoked axonal oxytocin release in
833 the central amygdala attenuates fear response. *Neuron* **73**, 553-566.
834
- 835 Kondratova AA & Kondratov RV. (2012). The circadian clock and pathology of the ageing
836 brain. *Nat Rev Neurosci* **13**, 325-335.
837
- 838 Kornhauser JM, Mayo KE & Takahashi JS. (1996). Light, immediate-early genes, and
839 circadian rhythms. *Behav Genet* **26**, 221-240.
840
- 841 Kruszynski M, Lammek B, Manning M, Seto J, Haldar J & Sawyer WH. (1980). [1-beta-
842 Mercapto-beta,beta-cyclopentamethylenepropionic acid),2-(O-methyl)tyrosine
843]argine-vasopressin and [1-beta-mercapto-beta,beta-cyclopentamethylenepropionic
844 acid]argine-vasopressine, two highly potent antagonists of the vasopressor response
845 to arginine-vasopressin. *J Med Chem* **23**, 364-368.
846
- 847 Landgraf R, Neumann I, Holsboer F & Pittman QJ. (1995). Interleukin-1 beta stimulates both
848 central and peripheral release of vasopressin and oxytocin in the rat. *Eur J Neurosci* **7**,
849 592-598.
850
- 851 LeGates TA, Fernandez DC & Hattar S. (2014). Light as a central modulator of circadian
852 rhythms, sleep and affect. *Nat Rev Neurosci* **15**, 443-454.
853
- 854 Li JD, Burton KJ, Zhang C, Hu SB & Zhou QY. (2009). Vasopressin receptor V1a regulates
855 circadian rhythms of locomotor activity and expression of clock-controlled genes in
856 the suprachiasmatic nuclei. *Am J Physiol Regul Integr Comp Physiol* **296**, R824-830.
857
- 858 Lucas RJ. (2013). Mammalian inner retinal photoreception. *Curr Biol* **23**, R125-133.
859
- 860 Luckman SM, Dyball RE & Leng G. (1994). Induction of c-fos expression in hypothalamic
861 magnocellular neurons requires synaptic activation and not simply increased spike
862 activity. *J Neurosci* **14**, 4825-4830.

863
864 Ludwig M & Leng G. (2006). Dendritic peptide release and peptide-dependent behaviours.
865 *Nat Rev Neurosci* **7**, 126-136.
866
867 Ludwig M, Sabatier N, Bull PM, Landgraf R, Dayanithi G & Leng G. (2002). Intracellular
868 calcium stores regulate activity-dependent neuropeptide release from dendrites.
869 *Nature* **418**, 85-89.
870
871 Marc RE & Jones BW. (2002). Molecular phenotyping of retinal ganglion cells. *J Neurosci*
872 **22**, 413-427.
873
874 Masland RH. (2001). The fundamental plan of the retina. *Nat Neurosci* **4**, 877-886.
875
876 Mieda M, Ono D, Hasegawa E, Okamoto H, Honma K, Honma S & Sakurai T. (2015).
877 Cellular clocks in AVP neurons of the SCN are critical for interneuronal coupling
878 regulating circadian behavior rhythm. *Neuron* **85**, 1103-1116.
879
880 Moritoh S, Sato K, Okada Y & Koizumi A. (2011). Endogenous arginine vasopressin-
881 positive retinal cells in arginine vasopressin-eGFP transgenic rats identified by
882 immunohistochemistry and reverse transcriptase-polymerase chain reaction. *Mol Vis*
883 **17**, 3254-3261.
884
885 Neumann ID & Landgraf R. (2012). Balance of brain oxytocin and vasopressin: implications
886 for anxiety, depression, and social behaviors. *Trends Neurosci* **35**, 649-659.
887
888 Paiva L, Sabatier N, Leng G & Ludwig M. (2016). Effect of Melanotan-II on brain Fos
889 immunoreactivity and oxytocin neuronal activity and secretion in rats. *J*
890 *Neuroendocrinol.* doi: 10.1111/jne.12454. [Epub ahead of print].
891
892 Paxinos G & Watson C. (2006). *The Rat Brain in Stereotaxic Coordinates*. San Diego, CA
893 Academic Press.
894
895 Pennartz CM, Bos NP, Jeu MT, Geurtsen AM, Mirmiran M, Sluiter AA & Buijs RM. (1998).
896 Membrane properties and morphology of vasopressin neurons in slices of rat
897 suprachiasmatic nucleus. *J Neurophysiol* **80**, 2710-2717.
898
899 Porterfield VM & Mintz EM. (2009). Temporal patterns of light-induced immediate-early
900 gene expression in the suprachiasmatic nucleus. *Neurosci Lett* **463**, 70-73.
901
902 Provencio I, Rodriguez IR, Jiang G, Hayes WP, Moreira EF & Rollag MD. (2000). A novel
903 human opsin in the inner retina. *J Neurosci* **20**, 600-605.
904
905 Reppert SM & Weaver DR. (2002). Coordination of circadian timing in mammals. *Nature*
906 **418**, 935-941.
907
908 Rusak B, Abe H, Mason R, Piggins HD & Ying SW. (1993). Neurophysiological analysis of
909 circadian rhythm entrainment. *J Biol Rhythms* **8 Suppl**, S39-45.
910
911 Sabatier N, Caquineau C, Dayanithi G, Bull P, Douglas AJ, Guan XM, Jiang M, Van der
912 Ploeg L & Leng G. (2003). Alpha-melanocyte-stimulating hormone stimulates

913 oxytocin release from the dendrites of hypothalamic neurons while inhibiting
914 oxytocin release from their terminals in the neurohypophysis. *J Neurosci* **23**, 10351-
915 10358.

916

917 Sabatier N, Richard P & Dayanithi G. (1998). Activation of multiple intracellular
918 transduction signals by vasopressin in vasopressin-sensitive neurones of the rat
919 supraoptic nucleus. *J Physiol* **513**, 699-710.

920

921 Saeb-Parsy K & Dyball RE. (2003). Responses of cells in the rat suprachiasmatic nucleus in
922 vivo to stimulation of afferent pathways are different at different times of the
923 light/dark cycle. *J Neuroendocrinol* **15**, 895-903.

924

925 Schmidt TM, Chen SK & Hattar S. (2011). Intrinsically photosensitive retinal ganglion cells:
926 many subtypes, diverse functions. *Trends Neurosci* **34**, 572-580.

927

928 Schmidt TM & Kofuji P. (2011). An isolated retinal preparation to record light response from
929 genetically labeled retinal ganglion cells. *JoVE* **47**.

930

931 Son SJ, Filosa JA, Potapenko ES, Biancardi VC, Zheng H, Patel KP, Tobin VA, Ludwig M
932 & Stern JE. (2013). Dendritic peptide release mediates interpopulation crosstalk
933 between neurosecretory and preautonomic networks. *Neuron* **78**, 1036-1049.

934

935 Stoop R. (2012). Neuromodulation by oxytocin and vasopressin. *Neuron* **76**, 142-159.

936

937 Subburaju S & Aguilera G. (2007). Vasopressin mediates mitogenic responses to
938 adrenalectomy in the rat anterior pituitary. *Endocrinology* **148**, 3102-3110.

939

940 Tobin VA, Hashimoto H, Wacker DW, Takayanagi Y, Langaese K, Caquineau C, Noack J,
941 Landgraf R, Onaka T, Leng G, Meddle SL, Engelmann M & Ludwig M. (2010). An
942 intrinsic vasopressin system in the olfactory bulb is involved in social recognition.
943 *Nature* **464**, 413-417.

944

945 Trudel E & Bourque CW. (2010). Central clock excites vasopressin neurons by waking
946 osmosensory afferents during late sleep. *Nat Neurosci* **13**, 467-474.

947

948 Tsuji T, Tsuji C, Ludwig M & Leng G. (2016). The rat suprachiasmatic nucleus: the master
949 clock ticks at 30 Hz. *J Physiol* **594**, 3629-3650.

950

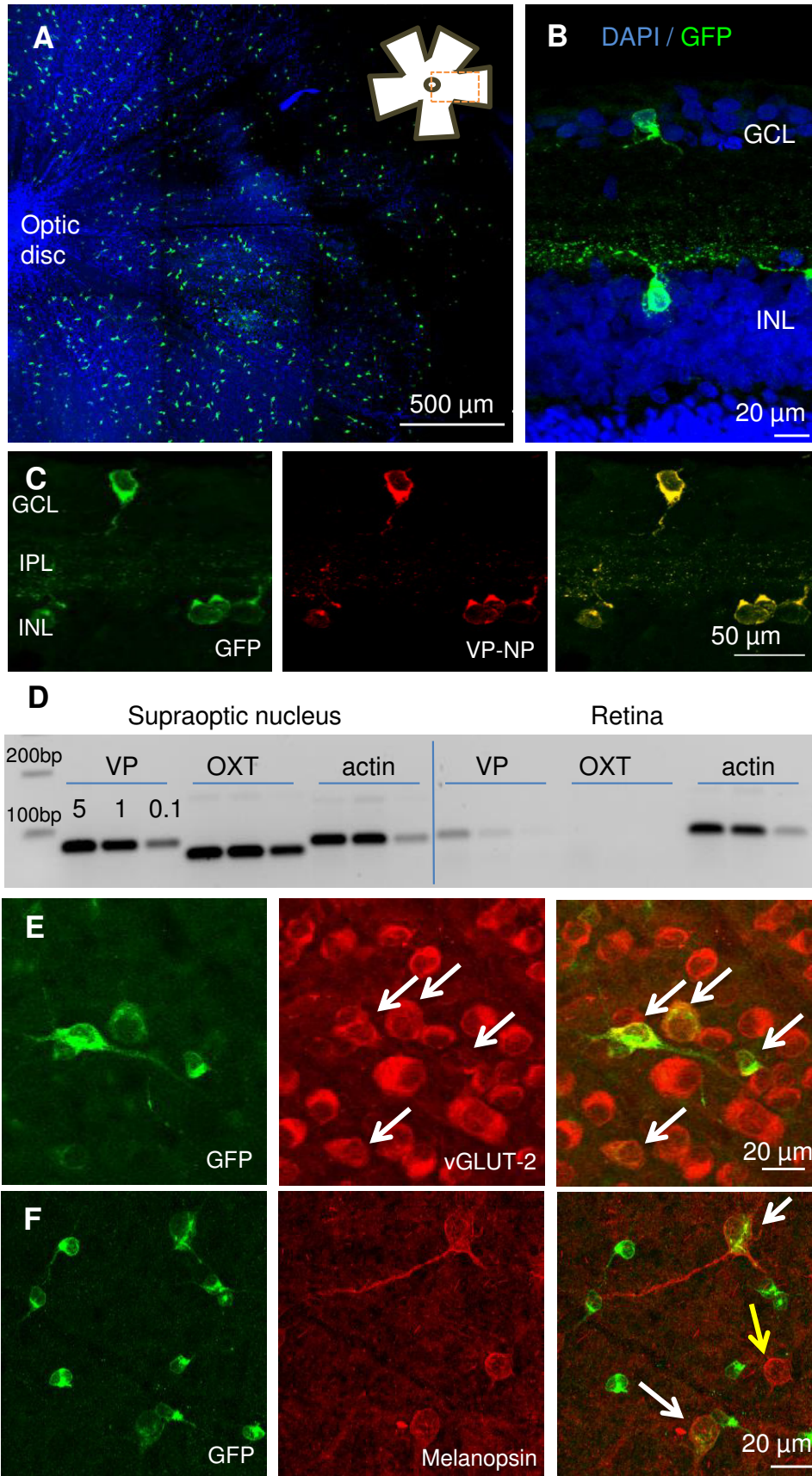
951 Ueta Y, Fujihara H, Serino R, Dayanithi G, Ozawa H, Matsuda K, Kawata M, Yamada J,
952 Ueno S, Fukuda A & Murphy D. (2005). Transgenic expression of enhanced green
953 fluorescent protein enables direct visualization for physiological studies of
954 vasopressin neurons and isolated nerve terminals of the rat. *Endocrinology* **146**, 406-
955 413.

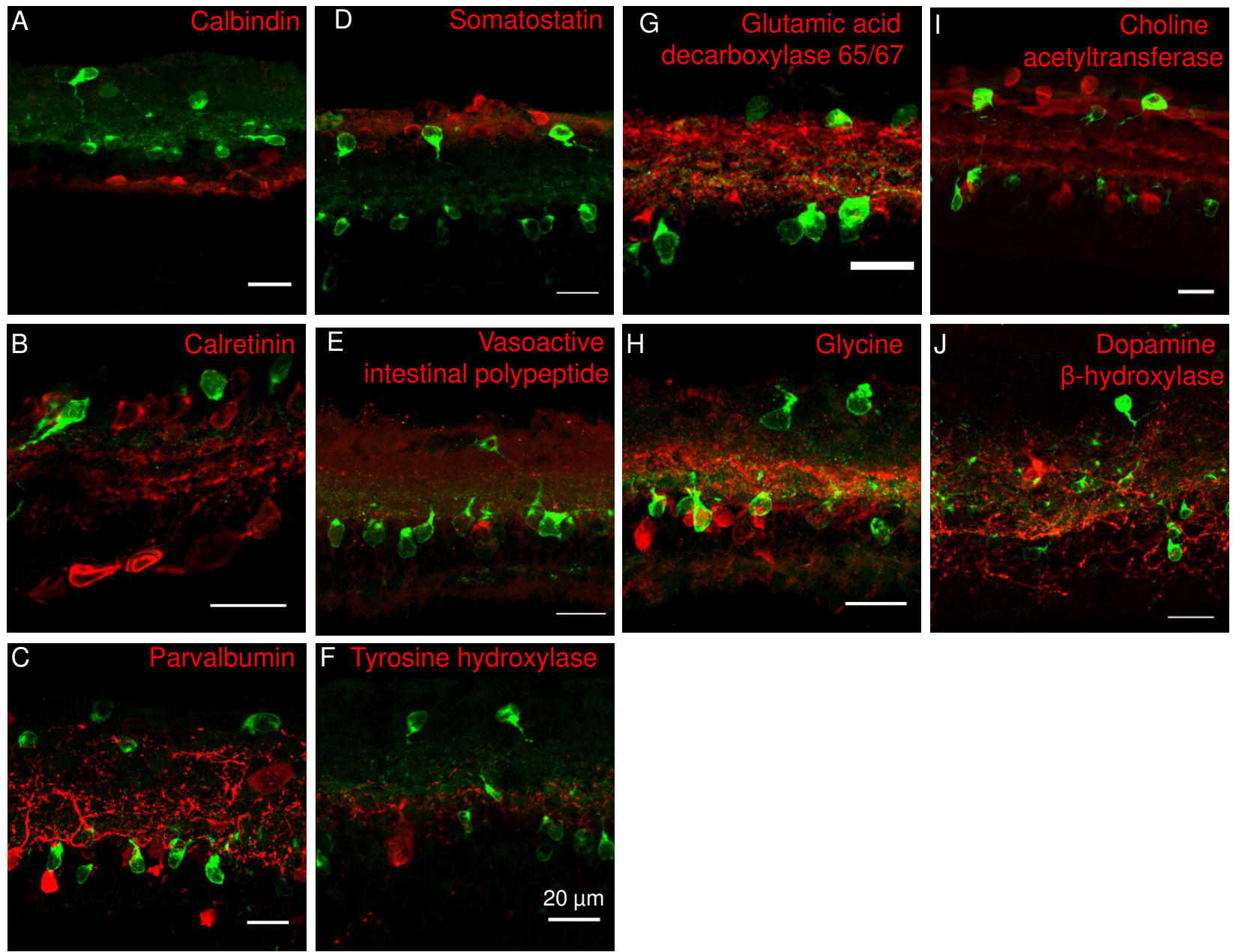
956

957 Yamaguchi Y, Suzuki T, Mizoro Y, Kori H, Okada K, Chen Y, Fustin JM, Yamazaki F,
958 Mizuguchi N, Zhang J, Dong X, Tsujimoto G, Okuno Y, Doi M & Okamura H.
959 (2013). Mice genetically deficient in vasopressin V1a and V1b receptors are resistant
960 to jet lag. *Science* **342**, 85-90.

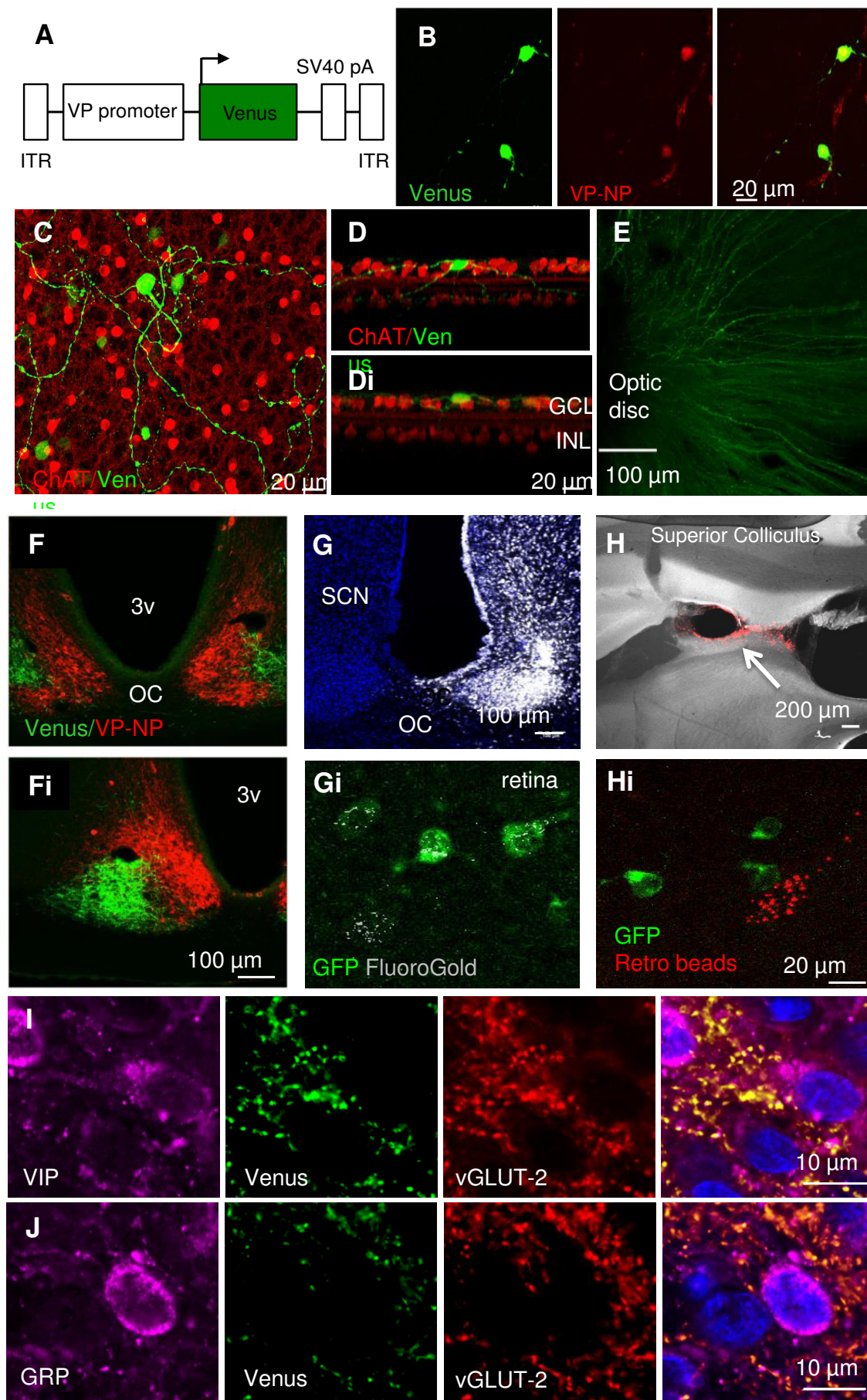
961

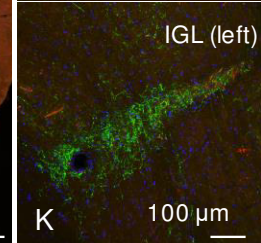
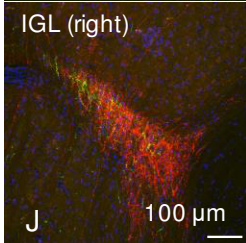
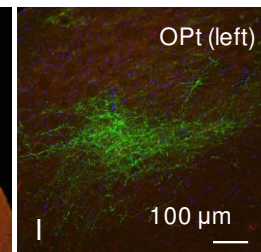
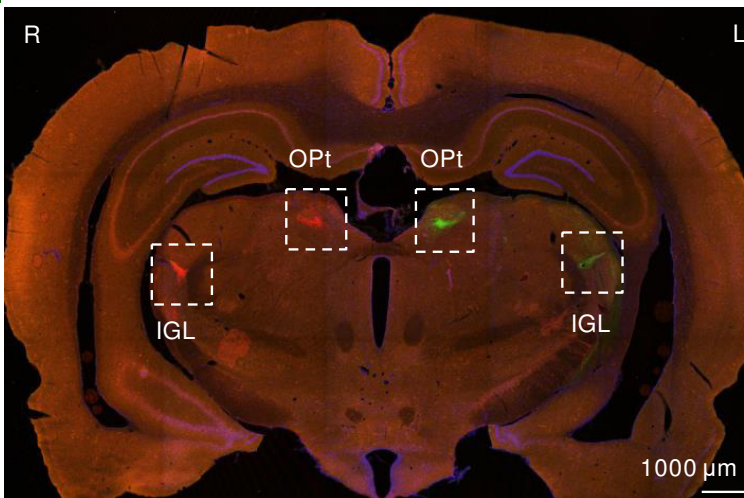
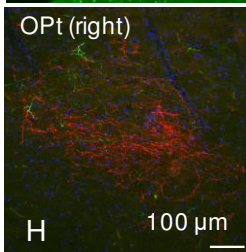
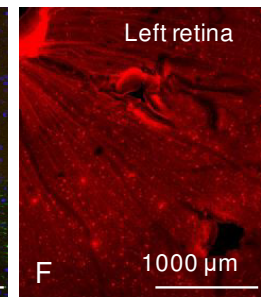
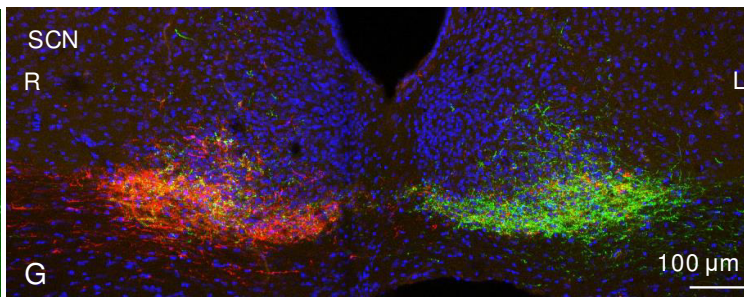
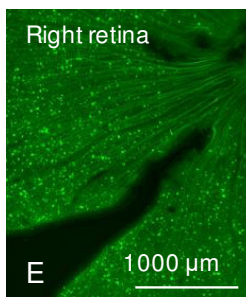
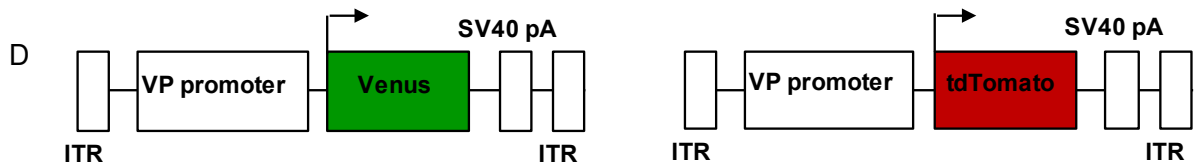
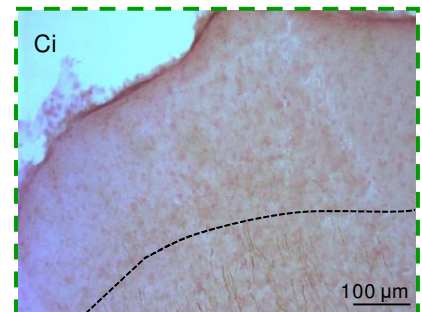
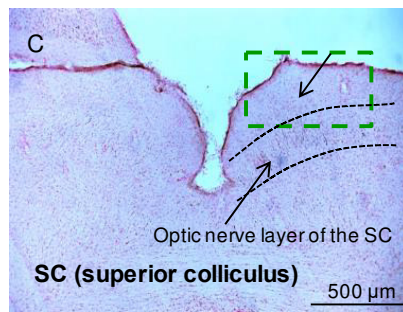
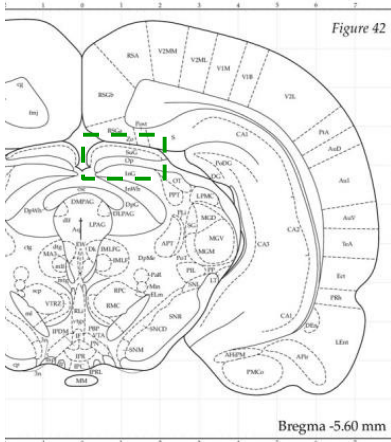
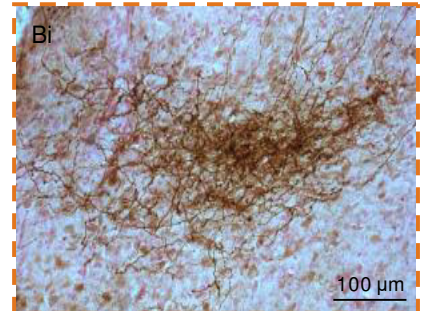
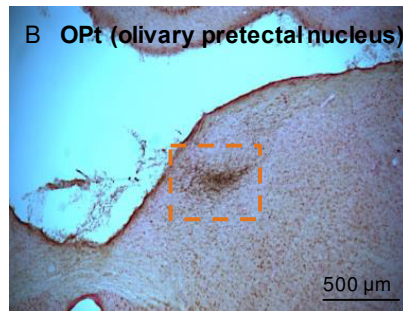
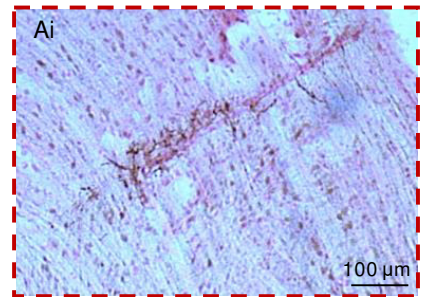
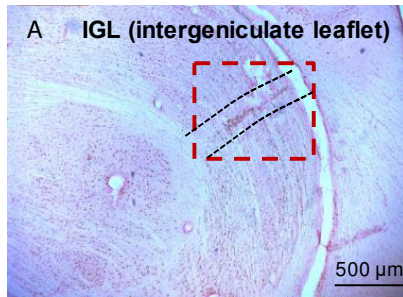
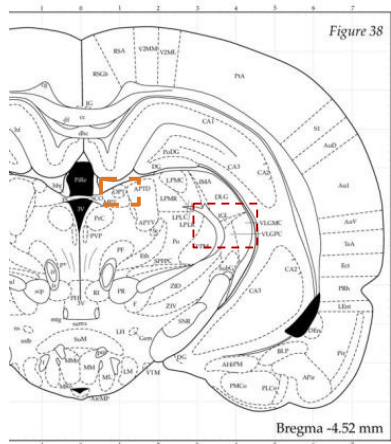
962

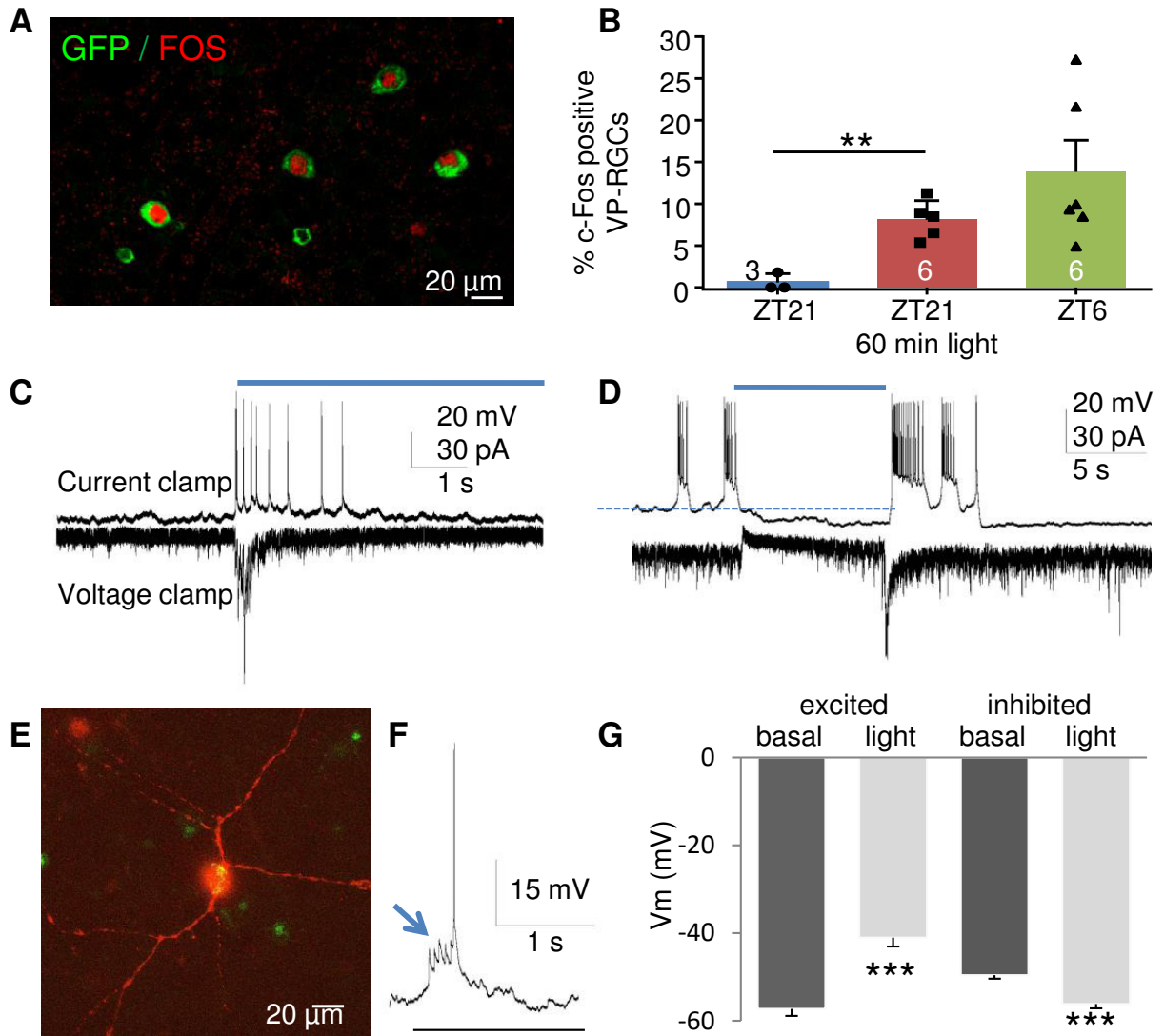


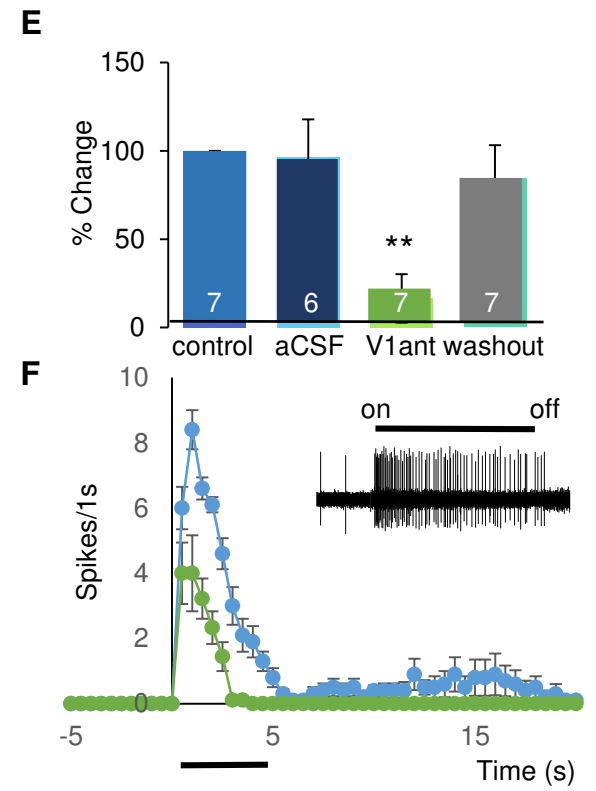
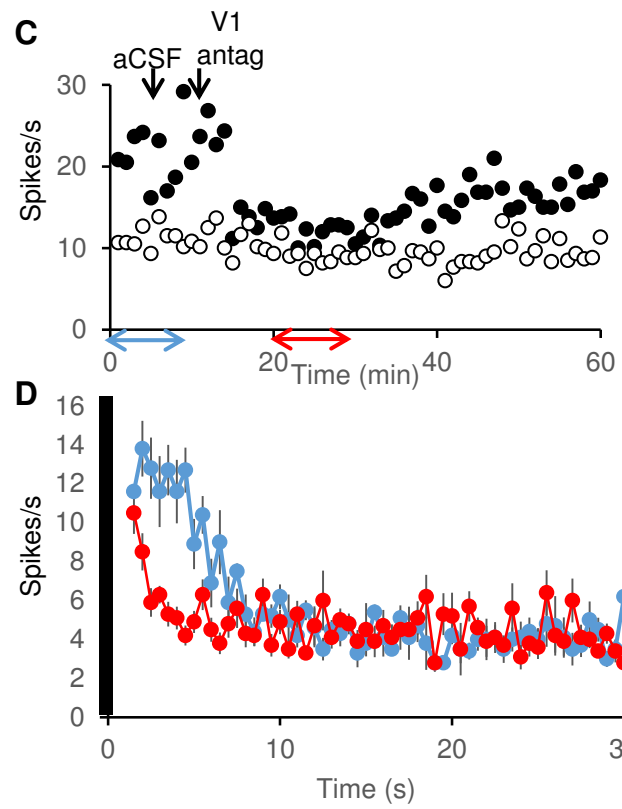
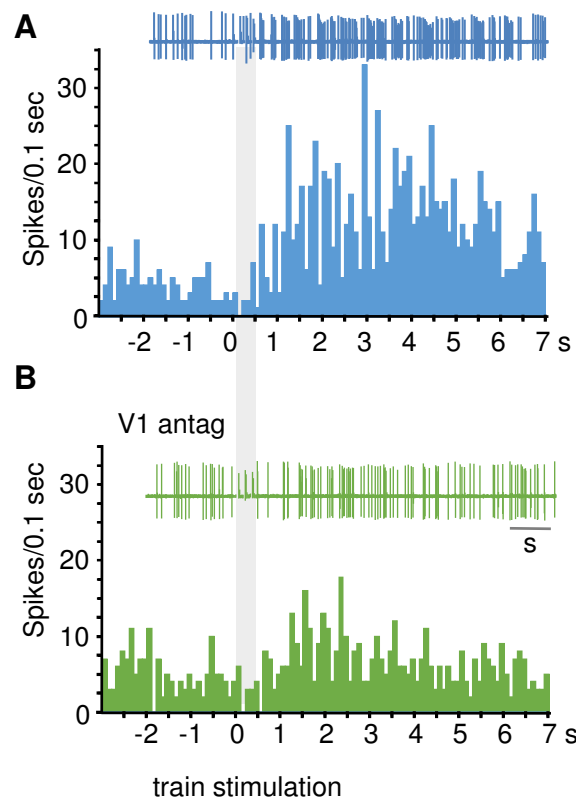


Tsuji et al., Figure 2









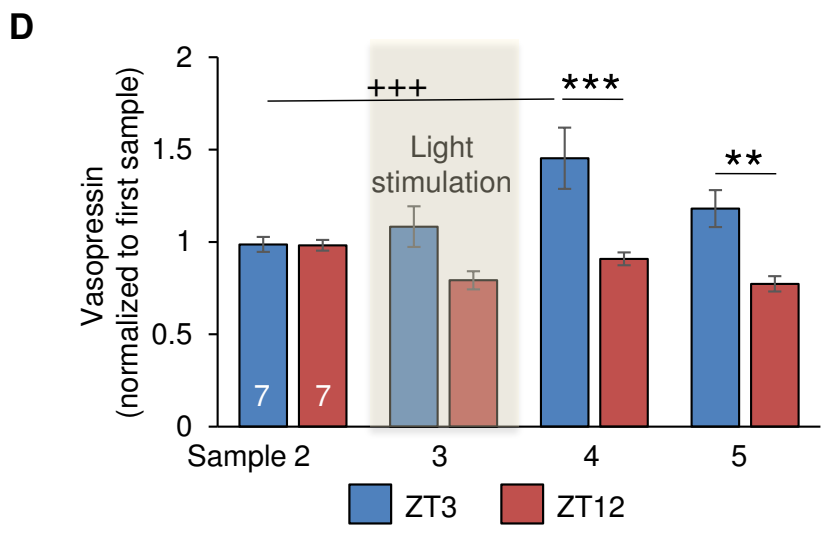
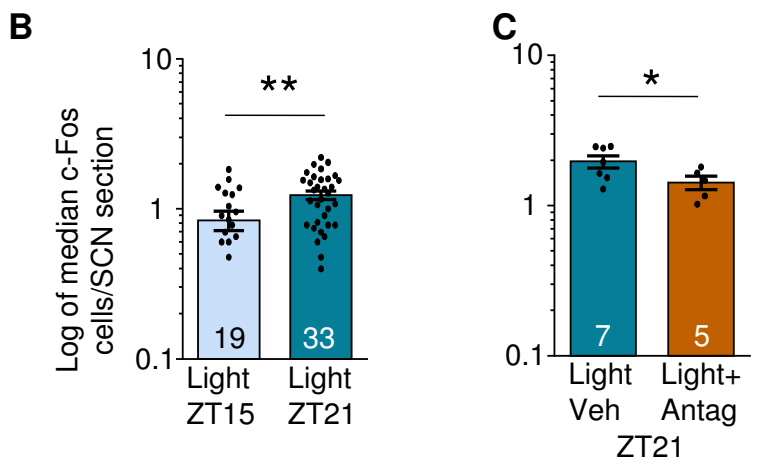
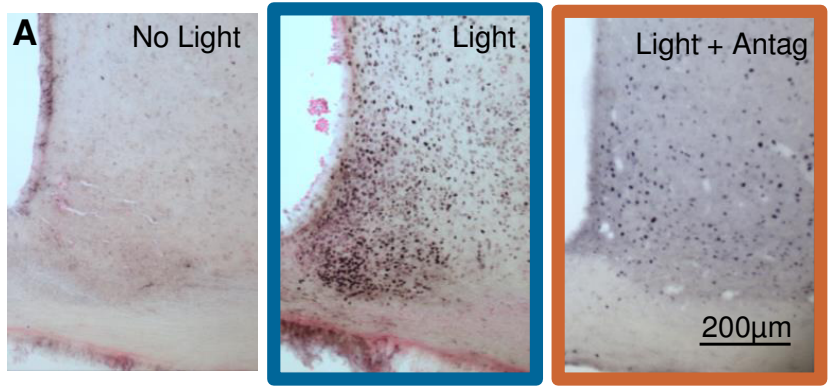


Table:**T1:** Primary antibodies used for retina and SCN immunohistochemistry

PRIMARY ANTIBODIES	CODE	SUPPLIER	DILUTION	HOST
eGFP	AB3080	Millipore, UK	1: 1000	rabbit
eGFP	MAB3580	Millipore, UK	1: 1000	mouse
Venus (GFP &YFP)	ab13970	Abcam, UK	1:15000	chicken
tdTomato	362496	Clontech	1:500	rabbit
Gastrin Releasing Peptide	ab43834	Abcam, UK	1:500	rabbit
Vasoactive Intestinal Peptide	20077	Immunostar, Newmarket Scientific, UK	1:500	rabbit
Melanopsin	AB19306	Abcam, UK	1:100	rabbit
Neuropeptide Y	22940	Immunostar, Newmarket Scientific, UK	1:500	rabbit
Somatostatin	20067	Immunostar, Newmarket Scientific, UK	1:500	rabbit
Vasopressin	PS41	Professor H Gainer (NIH, Bethesda, MD)	1:1000	mouse
Vasopressin	PC234L	Merck Chemicals Ltd. UK	1:200	rabbit
Calbindin D-28K	300	Swant, Switzerland	1:500	mouse
Calretinin	7699/3H	Swant, Switzerland	1:500	rabbit
Parvalbumin	24428	Immunostar, Newmarket Scientific, UK	1:500	rabbit
Glutamate Decarboxylase 65/67	ADI-MSA-225	Enzo Life Sciences (UK) LTD. Exeter, UK	1:1000	mouse
Vesicular Glutamate Transporter 2	135404	Synaptic Systems, Germany	1:1000	guinea pig
Glycine	AB5020	Millipore, UK	1:100	rabbit
Tyrosine Hydroxylase	AB152	Millipore, UK	1:1000	rabbit
Dopamine Beta Hydroxylase	AB1585	Millipore, UK	1:2000	rabbit
Choline Acetyltransferase	AB144P	Millipore, UK	1:1000	goat
Fos	PC38	Millipore, UK	1:20000	rabbit
Fos	226003	Synaptic Systems, Germany	1:100000	rabbit

T2: Secondary antibodies and visualization reagents used for retina and SCN immunohistochemistry

SECONDARY ANTIBODIES:	CODE	SUPPLIER	DILUTION	Host
Biotin-anti-rabbit IgG	BA-1100	Vector Laboratories Ltd, UK	1:500	horse
Biotin-anti-mouse IgG	BA-2001	Vector Laboratories Ltd, UK	1:500	horse
Biotin-anti-guinea pig IgG	BA-7000	Vector Laboratories Ltd, UK	1:500	goat
Biotin-anti-rabbit IgG	BA-1000	Vector Laboratories Ltd, UK	1:500	goat
Biotin-anti-mouse IgG	BA-9200	Vector Laboratories Ltd, UK	1:500	goat
Alexa 488 anti-chicken	A11039	Life Technologies, UK	1:500	goat
Biotin-Anti-Chicken IgY	703-066-155	Strattech Scientific Ltd, UK	1:500	donkey
VISUALISED WITH:				
Streptavidin, Alexa Fluor 488 conjugate	S-11223	Life Technologies, UK	1:500	
Streptavidin, Alexa Fluor 555 conjugate	S-21381	Life Technologies, UK	1:500	
Streptavidin, Alexa Fluor 647 conjugate	S-21374	Life Technologies, UK	1:500	